

THE CRYSTAL STRUCTURES OF
L- AND DL-LEUCINE

BY

R. MICHAEL HOWIESON

THESIS PRESENTED FOR THE DEGREE OF
MASTER OF PHILOSOPHY

University of Edinburgh

1974



SUMMARY

This thesis reviews the structures of alpha amino-acids which have been solved up to and including 1971, and gives the average intramolecular bond lengths and angles which are common to all amino-acids. Then follows a description of two related amino-acid structures.

L-Leucine forms very thin platelets which are monoclinic with space-group $P2_1$ and $Z = 4$. The cell dimensions are $a = 14.72 \text{ \AA}$, $b = 5.31 \text{ \AA}$, $c = 9.61 \text{ \AA}$, $\beta = 86.2^\circ$. The structure was solved by direct methods and refined to $R = 0.132$. Both molecules in the asymmetric unit exist as zwitterions, and each nitrogen atom is hydrogen bonded to 3 oxygen atoms. The molecules exist in double layers with the carboxyl and amino groups of two molecules pointing towards each other. The hydrocarbon ends of the molecules which face each other are only held by Van der Waal's forces, and this explains why the crystals form such thin platelets.

DL-Leucine also forms very thin platelets which are always twinned. The crystals are triclinic with space-group $P\bar{1}$ and $Z = 2$. The cell dimensions are: $a = 5.430 \text{ \AA}$, $b = 13.966 \text{ \AA}$, $c = 5.166 \text{ \AA}$, $\alpha = 96.7^\circ$, $\beta = 68.8^\circ$, $\gamma = 93.9^\circ$. The structure was solved by direct methods and refined to $R = 0.115$. The internal orientation and hydrogen bonding arrangement are very similar to those for L-leucine.

Appendix I describes some work done in assessing and developing the potential of a SAAB Mark II automatic film scanner which was just being brought into operation when this research started.

DECLARATION

I hereby declare that the work described in this thesis, and the composition of the same said thesis, were carried out by myself.

CONTENTS

	<u>Page</u>
 <u>CHAPTER 1</u>	
INTRODUCTION AND REVIEW OF ALPHA AMINO-ACID STRUCTURES	1-17
 <u>CHAPTER 2</u>	
THE CRYSTAL STRUCTURE OF L-LEUCINE	
2.1 Crystal Growth	19
2.2 Preliminary X-Ray Work	19
2.3 Space group and cell dimensions	20
2.4 Collection of 3-Dimensional Data	22
2.5 Absorption Corrections	22
2.6 Trial Structure	23
2.7 Refinement of Structure	29
2.8 Description of Structure	34
 <u>CHAPTER 3</u>	
THE CRYSTAL STRUCTURE OF DL-LEUCINE	
3.1 Crystal Growth	45
3.2 Preliminary X-Ray Work	45
3.3 Cell Dimensions and Space-group	47
3.4 Collection of 3-Dimensional Data	48
3.5 Absorption Corrections	51
3.6 Trial Structure	51
3.7 Refinement of Structure	53
3.8 Description of Structure	56
3.9 Conclusions	65

CONTENTS

	<u>Page</u>
<u>APPENDICES</u>	
<u>APPENDIX I</u> - The SAAB Mark II automatic film scanner	70
<u>APPENDIX II</u> - Observed and calculated structure factors for L-leucine	96
<u>APPENDIX III</u> - Observed and calculated structure factors for DL-leucine	105
<u>APPENDIX IV</u> - List of programs used from the X-Ray System '72	113
<u>APPENDIX V</u> - The Σ_1 formula	114
<u>REFERENCES</u>	115
<u>ACKNOWLEDGEMENTS</u>	118

CHAPTER 1

INTRODUCTION AND REVIEW OF ALPHA

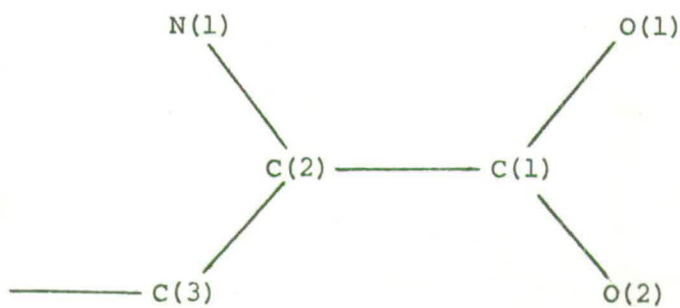
AMINO-ACID STRUCTURES

Amino-acids are the basic components of organic life, and are the building blocks from which proteins are made. Thus they are not only important in themselves, but their individual structures are very useful in determining those of proteins.

With the introduction of faster computers, more complex structures have been solved by x-ray crystallographic methods, with ever increasing accuracy. By 1948, only two-dimensional projections of very simple structures were being studied. Today, three-dimensional studies of proteins are becoming more and more commonplace. The peak of interest in amino-acids was from 1950-1960, and thus the majority of these structures have only been solved with intermediate accuracy (standard deviations being of the order of 0.01 \AA). Since then, the remaining gaps have gradually been filled in.

A fairly comprehensive review of amino-acid structures was produced by Marsh and Donohue in 1967 (1). They considered the native amino-acids, their hydrates, and their hydrohalides, and from the 37 compounds which came in these categories, they tabulated a set of bond lengths and angles which are common to all amino-acids (Table 1.1). As part of the initial work for this thesis, a survey of the literature from 1967-1971 showed that a further 27 structures had been solved, and a new enlarged set of bond lengths and angles was obtained which could be compared with the original one. The crystal data for these additional 27 structures is given in Table 1.2, whilst Tables 1.3 and 1.4 list the bond lengths and angles respectively. Table 1.5 shows the revised list of weighted mean bond lengths and angles for the amino-acid residue.

TABLE 1.1 Dimensions of the amino-acid residue as found by Marsh
and Donohue



By convention,

C(1) \equiv C

C(2) \equiv C $_{\alpha}$

C(3) \equiv C $_{\beta}$

Bonds:	C(1) - O(1)	1.252 Å
	C(1) - O(2)	1.253
	C(1) - C(2)	1.527
	C(2) - N(1)	1.487
	C(2) - C(3)	1.52

Angles:	O(1) - C(1) - O(2)	125.6°
	O(1) - C(1) - C(2)	118
	O(2) - C(1) - C(2)	116.4
	C(1) - C(2) - C(3)	111.5
	C(1) - C(2) - N(1)	110.5
	N(1) - C(2) - C(3)	110.5

TABLE 1.2 Amino-acid structures solved since the review of Marsh and Donohue.

(Bond lengths are in Å; bond angles in degrees)

Compound	Space Group	Z	a	b	c	β	Reference
ALANINE (β form)	Pbca	8	9.865	13.81	6.07		(2)
L-VALINE	$P2_1$	4	9.71	5.27	12.06	90.8	(3)
DL-VALINE	$P2_1/c$	4	5.21	22.10	5.41	109.2	(4)
L-VALINE.HCl	$P2_1$	2	10.394	7.072	5.430	91.42	(5)
L-VALINE.HCl.H ₂ O	$P2_1^2 2_1^2 2_1^2$	4	6.85	21.22	6.17		(6)
L-PROLINE	$P2_1^2 2_1^2 2_1^2$	4	11.55	9.02	5.20		(7)
DL-PROLINE.HCl	$P2_1/a$	4	12.49	6.71	8.70	93.42	(8)
L-LEUCINE.HI	$P2_1^2 2_1^2 2_1^2$	4	7.693	23.38	5.682		(9)
L-ASPARTIC ACID	$P2_1$	2	7.617	6.982	5.142	99.84	(10)
DL-ASPARTIC ACID	$C2/c$	8	19.06	7.48	9.29	123.95	(11)
L-GLUTAMIC ACID (β form)	$P2_1^2 2_1^2 2_1^2$	4	5.17	17.34	6.95		(12)
L-LYSINE.HCl.2H ₂ O	$P2_1$	2	7.492	13.320	5.879	97.79	(13)
L-HISTIDINE	$P2_1$	2	5.172	7.384	9.474	97.16	(14)
DL-HISTIDINE	$P2_1/c$	4	8.983	8.087	9.415	97.65	(15)

TABLE 1.2 (contd.)

Compound	Space Group	Z	a	b	c	β	Reference
DL-HISTIDINE.HCl.2H ₂ O	P2 ₁ /a	4	8.87	15.30	8.48	114.5	(16)
L-PHENYLALANINE.HCl	P2 ₁ ² ₁ ² ₁	4	27.68	6.98	5.34		(17) (18)
L-ARGININE.HCl.H ₂ O	P2 ₁	4	11.044	8.481	11.214	91.31	(19)
L-TRYPTOPHAN.HCl	P2 ₁	2	7.45	5.30	14.67	98.80	(20)
L-TRYPTOPHAN.HBr	P2 ₁	2	14.57	5.44	7.57	99.6	(20) (21)
L-CYSTEINE	P2 ₁	4	11.51	5.240	9.517	109.13	(22)
L-CYSTEINE.HCl.H ₂ O	P2 ₁ ² ₁ ² ₁	4	19.48	7.12	5.52		(23)
L-CYSTINE	P4 ₁	4	6.71	6.71	21.73		(24)
L-CYSTEIC ACID	P2 ₁ ² ₁ ² ₁	4	8.35	10.16	7.44		(25)
L-CYSTEIC ACID.H ₂ O	P2 ₁ ² ₁ ² ₁	4	6.927	19.027	5.305		(26)
L-GLUTAMINE	P2 ₁ ² ₁ ² ₁	4	16.01	7.76	5.10		(27)
DL-ORNITHINE.HBr	P2 ₁ /c	4	12.18	7.88	11.61	133.65	(28)
	P2 ₁ /c	4	9.39	7.9	11.66	109.83	(29)
L-ORNITHINE.HCl	P2 ₁	4	4.99	8.00	10.00	97	(30) (31)

TABLE 1.3 Bond lengths (in Å) of amino-acids listed in Table 1.2 (excluding those in the β form).
Standard deviations, where quoted, are given in parentheses.

Compound	C(1)-O(1)	C(1)-O(2)	C(1)-C(2)	C(2)-N(1)	C(2)-C(3)	Comments
L-VALINE	1.245(.012) 1.276(.014)	1.265(.016) 1.243(.017)	1.518(.014) 1.541(.014)	1.496(.016) 1.497(.016)	1.547(.015) 1.516(.015)	There are 2 independent molecules
DL-VALINE	1.248(.006)	1.249(.006)	1.527(.007)	1.483(.006)	1.541(.007)	
L-VALINE.HCl	1.200	1.309	1.509	1.495	1.558	
L-VALINE.HCl.H ₂ O	1.27(.017)	1.30(.017)	1.49(.021)	1.49(.018)	1.54(.021)	
L-PROLINE	1.28	1.26	1.52	1.53	1.52	
DL-PROLINE.HCl	1.239(.012)	1.323(.012)	1.519(.013)	1.473(.011)	1.543(.013)	
L-LEUCINE.HI	1.19 (.02)	1.30 (.02)	1.53 (.02)	1.53 (.02)	1.52 (.02)	
L-ASPARTIC ACID	1.252(.004)	1.242(.004)	1.543(.004)	1.495(.004)	1.518(.004)	
DL-ASPARTIC ACID	1.30 (.017)	1.22 (.017)	1.57 (.020)	1.50 (.018)	1.55 (.020)	
L-LYSINE.HCl.2H ₂ O	1.246(.004)	1.250(.004)	1.529(.003)	1.484(.004)	1.524(.003)	
L-HISTIDINE	1.247(.002) 1.214(.012)	1.250(.002) 1.252(.012)	1.545(.002) 1.553(.011)	1.493(.002) 1.479(.011)	1.536(.003) 1.534(.001)	There are 2 independent molecules
DL-HISTIDINE	1.248(.005)	1.252(.005)	1.529(.005)	1.482(.005)	1.537(.006)	
DL-HISTIDINE.HCl.2H ₂ O	1.235(.01)	1.262(.01)	1.515(.01)	1.504(.01)	1.545(.01)	
L-PHENYLALANINE.HCl	1.17 (.02)	1.34 (.02)	1.50 (.02)	1.48 (.02)	1.55 (.02)	
L-ARGININE.HCl.H ₂ O	1.235(.003)	1.258(.003)	1.544(.003)	1.490(.003)	1.517(.003)	

TABLE 1.3 (contd.)

Compound	C(1)-O(1)	C(1)-O(2)	C(1)-C(2)	C(2)-N(1)	C(2)-C(3)	Comments
L-TRYPTOPHAN.HCl	1.147(.013)	1.325(.013)	1.540(.013)	1.505(.014)	1.539(.013)	
L-TRYPTOPHAN.HBr	1.172(.020)	1.311(.020)	1.583(.020)	1.474(.018)	1.539(.020)	
L-CYSTEINE	1.25 (.012)	1.26 (.012)	1.51 (.013)	1.49 (.012)	1.52 (.014)	
L-CYSTEINE.HCl.H ₂ O	1.235(.021)	1.331(.021)	1.508(.023)	1.532(.017)	1.557(.023)	
L-CYSTINE	Not published					
L-CYSTEIC ACID	1.28 (.02)	1.22 (.02)	1.52 (.02)	1.51 (.02)	1.52 (.02)	Carboxyl group present as -COOH
L-CYSTEIC ACID.H ₂ O	1.220(.007)	1.287(.007)	1.510(.007)	1.497(.007)	1.532(.007)	
L-GLUTAMINE	1.22 (.024)	1.27 (.024)	1.52 (.024)	1.51 (.024)	1.50 (.024)	
DL-ORNITHINE.HBr	1.248(.02)	1.249(.02)	1.537(.02)	1.465(.02)	1.525(.02)	
L-ORNITHINE.HCl	1.245(.006)	1.257(.006)	1.541(.006)	1.497(.006)	1.529(.006)	

TABLE 1.4 Bond angles of amino-acids (in degrees) listed in Table 1.2 (excluding those in the β form) standard

deviations, where quoted, are given in parentheses

Compound	O(1)-C(1)-O(2)	O(1)-C(1)-C(2)	O(2)-C(1)-C(2)	C(1)-C(2)-C(3)	C(1)-C(2)-N(1)	N(1)-C(2)-C(3)
L-VALINE	124.8(1.0) 124.9(1.1)	117.7(.9) 116.0(1.0)	117.4(1.0) 119.1(1.0)	113.7(.9) 109.3(.9)	109.6(.9) 109.2(.9)	111.0(.9) 110.3(.9)
DL-VALINE	125.5(.4)	118.0(.4)	116.5(.4)	113.0(.4)	109.0(.4)	109.8(.4)
L-VALINE.HCl	123.9	123.7	112.4	114.5	106.2	109.8
L-VALINE.HCl.H ₂ O	122	123	115	110	108	114
L-PROLINE*	120.0	119.1	121.1	-	-	-
DL-PROLINE.HCl*	124.5(.9)	122.7(.8)	112.9(.8)	-	-	-
L-LEUCINE.HI	122(1)	126(1)	111(1)	113(1)	105(1)	106(1)
L-ASPARTIC ACID	127(1.5)	114(1.5)	111(1.5)	108(1.5)	112(1.5)	113(1.5)
DL-ASPARTIC ACID	126.8	114.1	118.9	108.3	111.9	112.9
L-LYSINE.HCl.2H ₂ O	125.5	117.7	116.8	109.8	109.7	111.8
L-HISTIDINE	126.7(.2) 127.4(.9)	117.1(.2) 117.1(.8)	116.3(.2) 115.4(.8)	110.6(.1) 109.6(.6)	109.5(.1) 109.5(.6)	109.8(.1) 111.4(.7)
DL-HISTIDINE	124.9(.3)	119.3(.4)	115.7(.3)	110.5(.3)	110.3(.3)	110.6(.3)
DL-HISTIDINE.HCl.2H ₂ O	126.3(.5)	118.3(.5)	115.4(.5)	108.3(.5)	109.1(.5)	109.2(.5)
L-PHENYLALANINE.HCl	124	127	116	113	106	112

TABLE 1.4 (contd.)

Compound	O(1)-C(1)-O(2)	O(1)-C(1)-C(2)	O(2)-C(1)-C(2)	C(1)-C(2)-C(3)	C(1)-C(2)-N(1)	N(1)-C(2)-C(3)
L-ARGININE.HCl.H ₂ O	126.3(.2)	118.5(.2)	115.2(.2)	111.0(.2)	109.9(.2)	111.8(.2)
L-TRYPTOPHAN.HCl	127.5(1.0)	125.7(.9)	106.8(.8)	115.0(.8)	107.0(.8)	109.7(.8)
L-TRYPTOPHAN.HBr	127.3(1.2)	124.7(1.2)	107.9(1.2)	116.2(1.2)	104.3(1.2)	112.4(1.2)
L-CYSTEINE	124.0(.8)	118.8(.8)	117.2(.8)	112.2(.8)	109.5(.8)	109.8(.8)
L-CYSTEINE.HCl.H ₂ O	122.0(1)	126.6(1)	111.4(1)	110.3(1)	105.2(1)	112.1(1)
L-CYSTINE	Not published					
L-CYSTEIC ACID	125(1)	115(1)	120(1)	110(1)	111(1)	111(1)
L-CYSTEIC ACID.H ₂ O	126.2(.4)	121.0(.4)	112.7(.4)	116.3(.4)	108.8(.4)	111.9(.4)
L-GLUTAMINE	128	116	116	111	114	110
DL-ORNITHINE.HBr	126.2(1.5)	116.9(1.5)	116.8(1.5)	108.3(1.5)	112.6(1.5)	109.6(1.5)
L-ORNITHINE.HCl	126.6(.4)	117.4(.4)	116.0(.4)	110.2(.3)	110.3(.3)	107.8(.3)

TABLE 1.5 The weighted mean bond lengths and angles for the amino-
acid residue determined from Tables 1.3 and 1.4

BONDS

		σ	Comment
C(1) - O(1)	1.230 Å	.016 Å	(a)
	1.245	.007	(b)
C(1) - O(2)	1.299	.017	(a)
	1.251	.005	(b)
C(1) - C(2)	1.539	.010	
C(2) - N(1)	1.491	.006	
C(2) - C(3)	1.530	.007	

ANGLES

		σ	Comment
O(1) - C(1) - O(2)	125.5°	1.4°	(a)
	126.3	0.5	(b)
O(1) - C(1) - C(2)	125.1	1.7	(a)
	117.7	0.7	(b)
O(2) - C(1) - C(2)	112.6	0.4	(a)
	115.8	0.8	(b)
C(1) - C(2) - C(3)	110.8	1.1	
C(1) - C(2) - N(1)	109.5	0.7	
N(1) - C(2) - C(3)	110.1	1.1	

Note: (a) Carboxyl group is in the form -COOH

(b) Carboxyl group is in the form -COO⁻

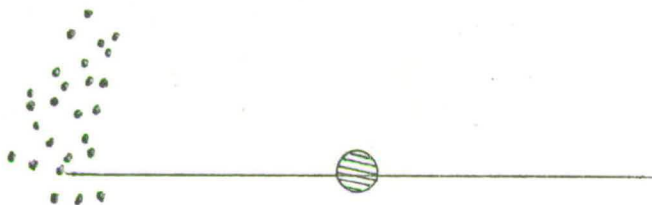
Table 1.6 Comparison of crystal data, bond lengths and bond angles
between L-leucine hydrobromide and L-leucine
hydroiodide.

	L-leucine hydrobromide	L-leucine hydroiodide
a	7.29 Å	7.693 Å
b	24.51	23.38
c	5.54	5.682
space-group	$P2_1^2_1^2_1$	$P2_1^2_1^2_1$
C(1) - O(1)	1.20 Å	1.19 Å
C(1) - O(2)	1.30	1.30
C(1) - C(2)	1.55	1.53
C(2) - N(1)	1.51	1.53
C(2) - C(3)	1.51	1.52
C(3) - C(4)	1.51	1.51
C(4) - C(5)	1.49	1.56
C(4) - C(6)	1.53	1.57
O(1) - C(1) - O(2)	124°	122°
O(1) - C(1) - C(2)	126	126
O(2) - C(1) - C(2)	110	111
C(1) - C(2) - C(3)	113	113
C(1) - C(2) - N(1)	105	105
N(1) - C(2) - C(3)	108	106
C(2) - C(3) - C(4)	119	114
C(3) - C(4) - C(5)	114	109
C(3) - C(4) - C(6)	111	108
C(5) - C(4) - C(6)	112	108

This enlarged set revealed that:

- (i) all bond lengths fall within the limits quoted by Marsh and Donohue.
- (ii) the angles at the carboxyl group, $C_{\beta}-C_{\alpha}-N$, and $C-C_{\alpha}-N$ are all fairly constant, with $C_{\alpha}-C-O(1)$ regularly being a little larger than $C_{\alpha}-C-O(2)$. There is no apparent reason for this, but the difference is a significant one. However, there is no significant difference between the two C-O bond lengths. The angles $C-C_{\alpha}-C_{\beta}$ and $C-C_{\alpha}-N$ do vary more than the others, and it is these angles which can most easily change to improve the hydrogen bonding and packing of the molecules.
- (iii) not all amino-acids exist in the zwitterion form as stated by Marsh and Donohue. In DL-proline hydrochloride (8), for example, the two C-O bond lengths are significantly different (1.239 Å and 1.323 Å).
- (iv) there is considerable variation in the dihedral angle about the $C-C_{\alpha}$ bond (Fig. 1.1). No apparent correlation appears to exist between the angle and the nature of either the carboxyl group or the nitrogen atom. The diagram, for the sake of clarity, does not show the position of the C_{β} atoms, which all lie very close to 120° anticlockwise from the nitrogen atom.
- (v) there is an approximately equal distribution in space groups between monoclinic and orthorhombic, the only exceptions being the γ -form of glycine (32) and L-cystine (33) which are hexagonal, the tetragonal form of L-cystine (24), and DL-leucine which is triclinic.
- (vi) as expected, hydrogen bonding plays a very important part in amino-acid structures. In the zwitterion form, $-NH_3^+$ is a good hydrogen bond donor, and $-COO^-$ is an excellent acceptor. Typical N...O lengths are 2.80-2.85 Å, and all three protons of the ammonium group are usually involved. In glycine (32) and L-lysine hydrochloride monohydrate (34), however, one of the protons forms a bifurcated hydrogen bond, and is shared equally between two acceptor atoms. Here the

FIG. 1.1 The conformation about the C(1) - C(2) bond
in amino-acids



Large dot = C(1) - C(2) bond

Line = carboxyl group

Small dots = projected positions of nitrogen atoms

N---O length is 3.0 Å.

Before going on to consider L- and DL-leucine, it is of interest to mention the more important features of the crystal structures of other amino-acids, both the L- and DL- forms of which have been solved, in order that comparisons can be made with the results obtained in this thesis.

L-Valine (3) has two independent molecules in the asymmetric unit, both of which exist in the zwitterion form (Fig. 1.2). Within experimental error, the two -COO^- groups are coplanar with their C_α atoms, and the $\text{C}_\alpha\text{-N}$ bonds deviate from these planes by 19.5° and 43.7° respectively. The two molecules have different conformations about the $\text{C}_\alpha\text{-C}_\beta$ bond. In one of these, the two hydrogen atoms are trans to each other, which had never been observed until that time. In DL-valine (4), once again, both molecules exist as zwitterions, but there is only one hydrogen bond from the nitrogen atom ($\text{N---O}(2) = 2.95 \text{ \AA}$). The C-N bond lies 21° out of the carboxyl plane, and the conformation about the $\text{C}_\alpha\text{-C}_\beta$ bond is the same for both molecules, namely the same as the common conformation found in L-valine.

L-Histidine (14) is shown diagrammatically in Fig. 1.3, and it is found that the imidazole ring is trans and fully staggered to the carboxyl group. In DL-histidine (15), the two groups are not fully staggered and make an angle of 150.9° about the $\text{C}_\alpha\text{-C}_\beta$ bond. Both the L- and DL- forms exist in approximately extended configurations, but they are far from identical as a comparison of the dihedral angles in Fig. 1.3 reveals. An examination of the hydrogen bonding and packing involved shows that:

- (i) the ammonium group always forms three hydrogen bonds.
- (ii) the imidazole nitrogen atoms always participate in one hydrogen bond.

FIG. 1.2 The zwitterion form of L-valine

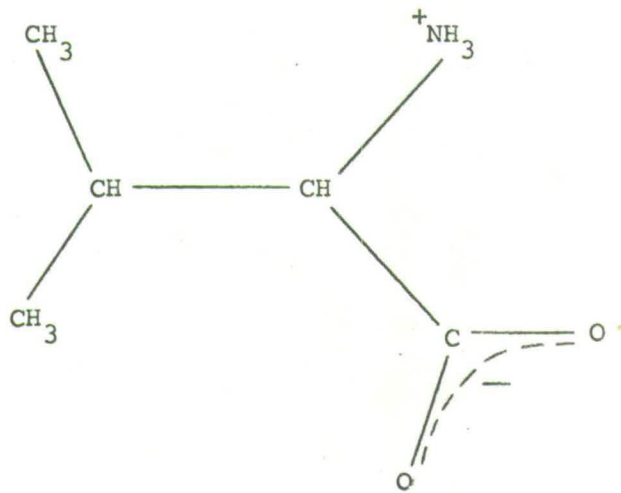
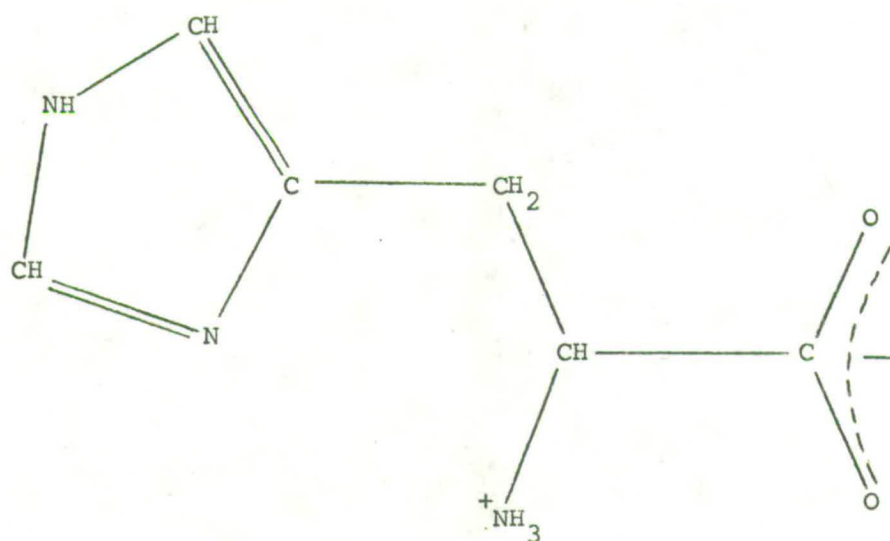


FIG. 1.3 The zwitterion form of an L-molecule, and the dihedral angles in L- and DL-histidine



	L-	DL-
O(2) - C(1) - C(2) - N(1)	154°	171°
C(1) - C(2) - C(3) - C(4)	180°	151°
C(2) - C(3) - C(4) - C(6)	-123°	114°

(iii) O(1) is involved in one hydrogen bond whereas O(2) is involved in two.

(iv) the molecules are very flexible (e.g. the variation in dihedral angles) and can easily adapt to their surroundings.

A survey of the literature showed that although neither L- or DL-leucine had had their crystal structures solved, a few related compounds had been analysed. The isomorphous pair of structures L-leucine hydrobromide (34) and L-leucine hydroiodide (9) have both been determined. For both these derivatives, the hydrogen atoms play an important part in the packing of the side-chains in the crystal. Only one intermolecular contact between side-chains is less than the expected Van der Waal's value, and side-chain atoms are found to have greater thermal motion than the polar ends. Because of the difference in polarizability between the two ends of the molecule, the number of efficient packing arrangements is limited, and the molecules pack in sheets perpendicular to the b -axis. The sheets are layered so that the hydrophobic side-chains are held together by Van der Waal's forces, and the polar ends held by hydrogen bonding forces. In both derivatives, the charged amino nitrogen atom undergoes rather weak hydrogen bonding with two halide atoms and one oxygen atom. A comparison of the crystal data, bond lengths and angles is given in Table 1.6.

In L-leucyl-L-prolyl-glycine (35), the average C-C bond length is 1.513 \AA which is significantly less than the more usual value of 1.54 \AA . The angle at C_{β} is 118° which is much higher than the expected tetrahedral angle of 109.5° . However, this seems to be a feature of other amino-acids and peptides where this angle consistently falls in the range $111-118^{\circ}$. It is thought that this is due to steric effects. This feature was also observed in glycyL-L-leucine (36) where the angle is 116.5° .

This thesis describes the determination of the crystal structures of L- and DL- leucine. Crystals of these compounds have been examined briefly by Moller (37) in 1949, but because techniques were not sufficiently sophisticated at that time, a full structure determination was not possible. From a study of the intensities and projected Patterson maps, he postulated that in both compounds the molecules lie approximately parallel to the longest axis, and pack in double layers with the polar ends of one layer pointing towards the polar ends of another. It would appear that the reason this work has not been followed up until now, is because of the difficulty in obtaining good single crystals. Both compounds crystallise as very thin plates, and in addition, DL-leucine is always twinned.

During this work, a SAAB Mark II automatic film scanner was being brought into use in this laboratory, and Appendix I describes some work connected with it.

CHAPTER 2

THE CRYSTAL STRUCTURE OF L-LEUCINE

2.1 Crystal Growth

Various methods were attempted in order to recrystallise the commercial sample obtained from BDH Chemicals Ltd., and the best results were obtained using isothermal distillation. Some of the impure crystals were dissolved in the minimum of cold water, and the vessel placed in a sealed desiccator, in the bottom of which was placed some ethanol. After about two weeks, the two liquids had partially diffused through the vapour phase, causing the amino-acid to crystallise out. The crystals so formed were extremely thin plates (usually about 0.02 mms. thick) which were very pliable. This made crystal shaping impossible if sharp reflections were to be obtained.

2.2 Preliminary X-Ray Work

A crystal was mounted on the end of a thin glass fibre and some preliminary oscillation and Weissenberg photographs were taken on a standard Pye Unicam Weissenberg camera mounted on a Philips PW1009 generator. The crystal had dimensions 0.44 x 0.14 x 0.025 mms., and was mounted so as to oscillate about its longest axis. The radiation used was Cu K_α with wavelength 1.5418 Å.

Oscillation photographs indicated an inter-layer spacing of 5.31 Å ('b' axis) and also mirror-plane symmetry (i.e. $I(hkl)=I(h\bar{k}l)$). The corresponding Weissenberg photographs showed 2 reciprocal axes of length 0.1050 reciprocal lattice units (r.l.u.) (a^*) and 0.1608 r.l.u. (c^*) containing an angle of 93.8°.

A second crystal was then similarly mounted, but oscillating about the 'c' axis. Its dimensions were 0.30 x 0.20 x 0.03 mms. Oscillation photographs indicated $c = 9.61$ Å, but mirror symmetry was absent. The corresponding Weissenberg photographs indicated

$b^* = 0.2905$ r.l.u. and reflections $Ok0$ (k odd) systematically absent.

Upper layer Weissenberg photographs showed no 'doubling' of festoons, indicating that the above dimensions were of the correct order.

2.3 Space-group and Cell Dimensions

The mirroring observed only for the 'b' axis oscillation indicated monoclinic symmetry, higher symmetry being eliminated since the corresponding zero-layer Weissenberg photograph had no axes at 90° or 60° to each other.

Observed conditions for reflection:

hkl : No conditions

$h0l$: No conditions

$Ok0$: $k = 2n$

\therefore space-group is $P2_1$

Due to the relatively poor quality of the crystals, it was impossible to obtain very accurate cell dimensions by measuring the splitting of spots at high angles of θ (Bragg angle), since the data did not go out that far. Thus dimensions had to be obtained by the less accurate method of using as many axial reflections as possible.

The calculations were carried out by means of a Wang electronic calculator containing a card program written by Dr. D.K. Fleming.

The program calculates reciprocal lattice cell translations from the inter-spot distances along any axial row on a zero-layer photograph.

The reciprocal lattice repeat distance is found from the formula

$\xi_1 = 2 \sin \theta / n$, where θ = Bragg angle, and n = order of the spot.

Hence θ requires to be expressed in terms of the distance from the $-n$ to the $+n$ spot, as measured along the axial row.

If T = camera translation for 180° rotation of crystal

D = film diameter

l_n = spot to corresponding spot distance, along the axial row, for the n^{th} order,

then

$$\theta = \frac{l_n}{2 \sqrt{\frac{T^2}{\lambda^2} + D^2}}$$

From the above calculations, the following real and reciprocal cell dimensions were obtained:

$$a^* = 0.1050 \text{ r.l.u.} \qquad a = 14.72 \text{ (.08) \AA}$$

$$b^* = 0.2905 \qquad b = 5.31 \text{ (.08)}$$

$$c^* = 0.1608 \qquad c = 9.61 \text{ (.08)}$$

$$\beta^* = 93.8^\circ \qquad \beta = 86.2^\circ$$

Errors quoted are estimated standard deviations.

The density of the crystals as measured by the flotation method was found to be 1.14 gm.cm⁻³

$$\text{Cell volume, } V = abc \sin \beta = 749.4 \text{ \AA}^3$$

Hence the number of molecules per unit cell is given by:

$$Z = \frac{V \times \rho \times N_0}{F \times 10^{24}} = 3.9 \approx 4$$

Where N_0 = Avogadro's Number

and F = Formula weight.

Note: The cell dimensions quoted above do not follow the conventional system of having $\beta > 90^\circ$. If the other system is required to be used, then the reflection data must be modified by changing 2 of the 3 indices for all reflections (e.g. I(hkl) becomes I(\bar{h} kl)). A further note on how to convert the atomic co-ordinates will be made later.

2.4 Collection of 3-Dimensional Data

The crystal which was mounted about the b-axis was now used to collect 3-dimensional data on Kodak Kodirex film by the equi-inclination Weissenberg technique. Layers 0-4 inclusive were recorded using two film packs of 3 films each for each layer, exposure times differing by a factor of 16. In a similar manner, the second crystal, mounted about the c-axis, was used to collect layers 0-6 inclusive along this axis. Throughout the data collection the camera, generator and radiation used were as mentioned in 2.2.

The reflection intensities were measured visually using an intensity strip. As the relevant computer software was not sufficiently advanced at this stage, the SAAB film scanner was not used in this structure determination.

Total number of reflections accessible	960
Number of reflections with measurable intensity	771
Number of reflections too weak to measure	189

The intensities were corrected for Lorentz and polarisation factors before being scaled together.

A listing of the observed and calculated structure factors is given in Appendix II.

2.5 Absorption Corrections

Since the quality of this data was not as high as might have been desired, and as there were no atoms present in the molecule with a scattering power greater than oxygen, it was decided that it would be meaningless to apply these corrections. (Linear absorption coefficient = 6.2 cm^{-1}).

2.6 Trial Structure

Since there were no heavy atoms present in the molecule, it was decided to attempt to solve the structure using direct rather than Patterson methods.

The reflection data was first normalised using the program NORM (P. Main, M.M. Woolfson, G. Germain: University of York) which set up a file containing indices and their associated E factors, which were calculated from:-

$$|E_{hkl}| = \frac{|F_{hkl}| \times D}{\{P \times \sum F_j^2\}^{1/2}}$$

where D = F relative scale factor correction to ensure that the average value of $|E|^2 = 1.0$

F_j = the J^{th} scattering factor at the appropriate $\sin \theta/\lambda$ value for the reflection

P = correction factor allowing for space-group symmetry.

Table 2.1 shows that a statistical analysis of these E values confirms that the space-group is acentric.

These modified structure factors were then used as input for MULTAN (P. Main, M.M. Woolfson, G. Germain: University of York).

It is based on the tangent formula of Karle and Hauptman (38), and is in three parts which may be run separately or in combination.

(i) SIGMA2

This section of the program sets up all Σ_2 phase relationships of the form:

$$\phi_{\underline{h}} \approx \phi_{\underline{h}'} + \phi_{\underline{h}-\underline{h}'}, \quad \text{where } \phi_{\underline{h}} = \text{phase of } F_{\underline{h}}.$$

In order to save storage space and computing time, only the strongest relationships are retained and used by the tangent formula.

TABLE 2.1

Statistical analysis of normalised structure factors to determine whether space-group is centric or not.

	Experimental	Theoretical	
		Centric	Acentric
Average E^2	1.0000	1.0000	1.0000
Average $ E^2-1 $	0.7748	0.9680	0.7360
Average $ E $	0.8740	0.7980	0.8860

(ii) CONVERGE

In this part, the space-group information passed on from SIGMA2 is used to determine the types of reflections required to define the origin. It also determines the Σ_1 formula (Appendix V) which is applicable to the space-group concerned, and the restrictions placed on the phase values by space-group symmetry, i.e. whether a phase is restricted to values of 0, Π , or $\pm\Pi/2$.

When applying the Σ_1 formula, the program computes probabilities for the signs of centric reflections which are also structure invariants. For the present set of data, all reflections were used in calculating the Σ_1 formula, and the sign of a reflection's phase was accepted if the probability was greater than 0.900.

In addition, CONVERGE determines the best reflections for origin and enantiomorph definition and finds a small number of other reflections which appear to provide a good starting point for phase determination. For space-group $P2_1$, suitable reflections for defining origin and enantiomorph are two $h0l$ and one hll reflections, as these are subject to phase restrictions.

In choosing a suitable starting set, one is chosen which uses the strongest phase relationships and leads quickly to multiple indications for unknown phases, thus increasing the reliability of phase determination during the initial crucial stages. Such a starting point is found using the following formula:-

$$\alpha_h^2 = \sum_{h'} K_{hh'}^2 + 2 \sum_{\substack{h' \\ h' \neq h''}} \sum_{h''} K_{hh'} K_{hh''} \frac{I_1(K_{hh'}) I_1(K_{hh''})}{I_0(K_{hh'}) I_0(K_{hh''})} \quad (39)$$

where α_h = measure of the reliability of phase ϕ_h

$K_{hh'}$ = a weighting factor

I_1 = a modified Bessel function.

The value of α_h is estimated for all reflections, and the reflection with the smallest estimated α_h is eliminated from the data set, together with all the phase relationships in which the reflection is involved. Having eliminated these relationships, α_h is then recalculated for all remaining reflections and the new smallest α_h is eliminated. By this repeating process, the program converges on the group of reflections which are linked together with a large number of strong phase relationships and so will form a good starting point for phase determination. The results of applying CONVERGE to L-leucine are shown in Table 2.2 where the starting reflections are listed, together with the best phases as found by FASTAN.

(iii) FASTAN

The tangent formula section of the program generates each starting set of phases by assigning phase values in quadrants to those reflections chosen by CONVERGE, and develops them into a complete set of phases using the phase relationships output by SIGMA2.

Phases are determined and refined using a weighted tangent formula (40):

$$\tan \phi_h = \frac{\sum_{h'} w_{h'} w_{h-h'} |E_{h'} E_{h-h'}| \sin(\phi_{h'} + \phi_{h-h'})}{\sum_{h'} w_{h'} w_{h-h'} |E_{h'} E_{h-h'}| \cos(\phi_{h'} + \phi_{h-h'})} = \frac{T_h}{B_h}$$

where w_h = weight associated with the phase ϕ_h . Each weight is computed from

$$w_h = \tan h(\frac{1}{2}\alpha_h)$$

and $\alpha_h = |E_h| (T_h^2 + B_h^2)^{\frac{1}{2}}$

TABLE 2.2

Starting reflections with phases of trial set as found by MULTAN

(i) Reflections with fixed phase values:

<u>Reflection</u>	<u>Phase</u>
8 0 4	0
0 0 6	180

(ii) Reflections defining the origin

<u>Reflection</u>	<u>Phase</u>
0 1 3	45
1 1 5	45
3 4 -3	0

(iii) Other reflections found by CONVERGE:

<u>Reflection</u>	<u>Phase</u>
5 0 0	0
7 1 7	135
2 4 3	45

Since the tangent formula is weighted, all reflections are included the whole of the time, and there is no rejection criterion for a phase other than the weight being calculated as very small or zero. This form of weighting ensures that poorly determined phases have little effect in the determination of other phases, while the fact that all phases are included in the phase determination process leads to very efficient propagation of known phases throughout the data set.

For each set of phases determined, 3 figures of merit are calculated:-

- (a) ABS FOM - this is related to $\Sigma \alpha_h$, and is a measure of the internal consistency of the set of phases. For the correct set of phases a value of 1.2 or greater is obtained.
- (b) PSI ZERO - this was first defined by Cochran and Douglas (41)

$$\psi_0 = \sum_h \left| \sum_{h'} E_{h'} E_{h-h'} \right|$$

The terms in the inner summation are all those for which phases are known, and the values of h in the outer summation are those for which $|E_h|$ is either very small or zero. Thus for the correct set of phases, ψ_0 is a minimum.

- (c) RESID - this is merely an ordinary crystallographic residual for the equations

$$E_h = K \langle E_{h'} E_{h-h'} \rangle_{h'}$$

where K is a scale-factor. As for ψ_0 , RESID should be a minimum for the correct phases, but the latter is not as good an indicator as ψ_0 .

On applying the present set of data to FASTAN, the program produced 2 sets of phases with good figures of merit and differing only in that starting

reflection 2 5 0 was assigned a phase of 0 in one set, and π in the other. The actual figures of merit obtained for the former set are listed in Table 2.3. From this set, a 3-dimensional E-map was obtained. The peaks were plotted on a model and their contact distances calculated using BONDLA. By comparing these two, 13 peaks were assigned to atoms as a starting point to the solution. Their co-ordinates are listed in Table 2.4. Fig. 2.1 shows the numbering system used in the molecule.

2.7 Refinement of Structure

In order to carry out the various computer calculations involved, use was made of the collection of inter-related Fortran [?]prams known as the X-RAY system (1972 version). The system was edited by J.M. Stewart, G.J. Kruger, H.L. Ammon, G. Dickinson and S.R. Hall at the Computer Science Centre, University of Maryland. The programs could be used individually, or run consecutively in any order decided by the user. Appendix IV gives a list of the programs used during the various stages of the solution of the structure.

As a starting point, plausible peaks from the E-map were used as atom positions, 13 of which were input into the system via LOADAT, while reflection, space-group and cell data were input via DATRDN. Scattering factors for C, N, H and O atoms were supplied automatically by the system using those calculated from Hartree-Fock wave functions (42). Using isotropic temperature factors, calculated structure factors were calculated using the program FC, and this gives a residual factor $R = 0.485$ where R has the usual crystallographic definition, namely:

$$R = \frac{\sum | |F_o| - |F_c| |}{\sum |F_o|}$$

TABLE 2.3

Figures of merit for the best starting set of phases.

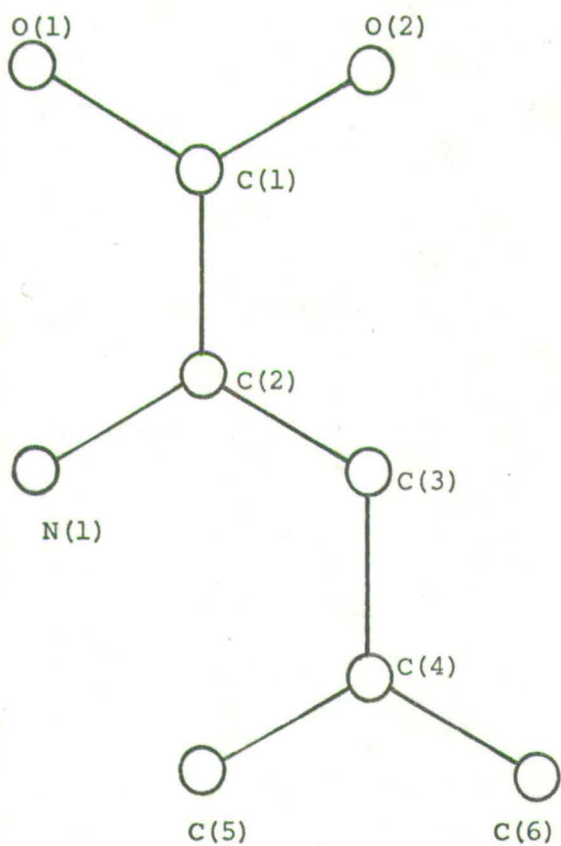
ABS FOM	=	1.1941
PSI ZERO	=	0.0
RESID	=	28.09

TABLE 2.4

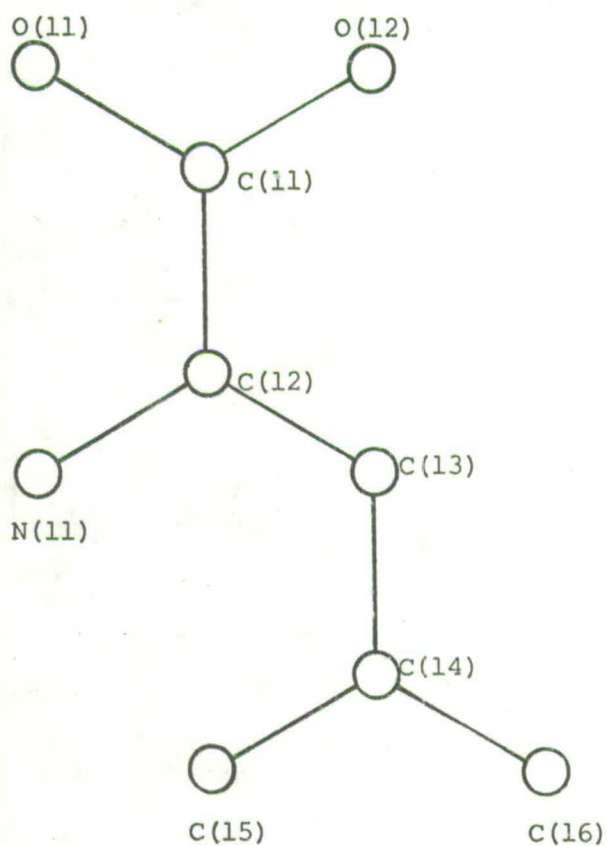
Fractional co-ordinates of atoms used for trial structure.

<u>ATOM</u>	x	y	z
O(2)	0.405	0.50	0.158
N(1)	0.409	0.75	0.396
C(1)	0.375	0.42	0.250
C(2)	0.355	0.50	0.379
C(3)	0.250	0.58	0.379
C(4)	0.216	0.32	0.417
O(12)	0.588	0.64	0.342
N(11)	0.575	0.75	0.104
C(11)	0.614	0.50	0.271
C(13)	0.730	0.73	0.100
C(14)	0.790	0.50	0.100
C(15)	0.800	0.31	1.000

Fig. 2.1 Numbering system of atoms within the two molecules



Molecule A



Molecule B

N.B. excluding hydrogen atoms

where F_o = observed structure factor

and F_c = calculated structure factor. This seemed a reasonable R value to begin work on (c.f. $R = 0.59$ for random positions).

The structure was then improved by moving atoms within the cell to new positions as indicated by observed and difference Fourier maps (using the program FOURR). By this technique, the residual factor was lowered to $R = 0.381$.

At this stage, the structure was thought to be sufficiently accurate to complete it by least squares refinement. To this end, CRYLSQ was used. Full matrix least squares methods were adopted throughout, but at first only an overall isotropic temperature factor of $B = 4.0$ was used, where $B = 8\pi^2 u^2$ where u^2 = mean square of the amplitude of atomic vibration. When $R < 0.30$ however, CRYLSQ modified the temperature factors allocating individual isotropic factors which were refined during each cycle. In addition, the scale-factors between the various layers of reflection data were also refined by the program. Refinement was continued down to $R = 0.156$.

At this stage, the refinement was continued by allowing the temperature factors of all atoms to refine anisotropically, at the same time restricting the individual layer scale-factors to be refined together and not separately. This further reduced R to 0.132 . In order to find possible sites for hydrogen atoms, use was made of the program BOND (Dr. R.O. Gould) which calculates, among other things, the theoretical position of an atom knowing the distance and angles from another group of atoms. By comparing these co-ordinates with the difference Fourier map, a set of atomic parameters for all 26 hydrogen atoms was obtained. As a further check, all bond distances and angles were calculated to confirm the positions were sensible.

A list of the final calculated and observed structure factors, not including hydrogen atoms, but with all other atoms anisotropic, is given in Appendix II.

2.8 Description of Structure

Final positional parameters of all atoms in the asymmetric unit, including hydrogen atoms, are given in Table 2.5. Table 2.6 lists the anisotropic temperature factors for the non-hydrogen atoms, whilst Table 2.7 gives the bond distances and angles within the two independent molecules. By comparing with the updated dimensions obtained for other amino-acids (Table 1.5) it can be seen that there are no significant differences, however some of the bonds, such as C(1)-C(2), C(2)-C(3), C(4)-C(6), C(14)-C(15) and C(14)-C(16), and angles, such as C(3)-C(4)-C(5) and C(13)-C(14)-C(15), all differ considerably from the more accepted values. It is thought that these are most probably due to some systematic error in the data, which being collected by the visual method was less accurate than the data collected by the SAAB scanner for DL-leucine. In order to confirm this, some of the more offending atoms, such as C(2) and C(6) were moved to new positions which gave more reasonable dimensions. As a result, the R factor increased, and on application of least squares, these atoms returned to their former positions with a corresponding drop in the R factor.

Fig.2.2 shows the projection of the structure looking down the b-axis. The two independent molecules lie approximately parallel to the a-axis with the carboxyl ends facing each other in order to facilitate hydrogen bonding. The conformation angles of the two molecules are shown in Table 2.8, and it can be seen that each pair of corresponding angles agrees to within 10° , showing how similar the two conformations are.

As with other amino-acids, the molecules exist in the zwitterion form, that is to say every nitrogen atom has three hydrogen atoms attached to it, and the two C-O bond distances are not significantly different from each other within one molecule. The equations of the planes through

TABLE 2.5

Final positional parameters of L-leucine. Errors in parentheses are estimated standard deviations.

<u>ATOM</u>	x	y	z
O(1)	0.414(1)	0.558(3)	0.153(1)
O(2)	0.382(1)	0.171(5)	0.235(1)
N(1)	0.406(1)	0.747(4)	0.410(1)
C(1)	0.388(1)	0.400(5)	0.243(2)
C(2)	0.349(2)	0.522(5)	0.389(2)
C(3)	0.256(1)	0.601(5)	0.386(2)
C(4)	0.188(2)	0.384(7)	0.391(3)
C(5)	0.184(2)	0.228(7)	0.521(3)
C(6)	0.086(2)	0.474(9)	0.353(3)
O(11)	0.585(1)	0.624(3)	0.360(1)
O(12)	0.636(1)	0.253(4)	0.271(1)
N(11)	0.572(1)	0.835(4)	0.111(1)
C(11)	0.618(1)	0.481(4)	0.265(2)
C(12)	0.636(1)	0.613(4)	0.121(2)
C(13)	0.731(1)	0.713(5)	0.104(2)
C(14)	0.803(2)	0.504(5)	0.093(2)
C(15)	0.806(2)	0.355(6)	-0.031(3)
C(16)	0.904(2)	0.646(7)	0.097(3)
H(C2)	0.359	0.395	0.465
H(C3)	0.238	0.715	0.473
H(C3)	0.246	0.710	0.301
H(C4)	0.212	0.266	0.313
H(C5)	0.077	0.669	0.388
H(C5)	0.080	0.483	0.250
H(C5)	0.034	0.373	0.402
H(C6)	0.243	0.234	0.562
H(C6)	0.152	0.072	0.503
H(C6)	0.136	0.350	0.583
H(N1)	0.380	0.888	0.358
H(N1)	0.406	0.783	0.512

TABLE 2.5 (contd.)

<u>ATOM</u>	x	y	z
H(N1)	0.471	0.717	0.373
H(C12)	0.624	0.488	0.042
H(C13)	0.740	0.822	0.015
H(C13)	0.743	0.827	0.186
H(C14)	0.792	0.393	0.177
H(C15)	0.741	0.372	-0.067
H(C15)	0.818	0.175	-0.011
H(C15)	0.830	0.454	-0.115
H(C16)	0.950	0.500	0.125
H(C16)	0.899	0.773	0.180
H(C16)	0.922	0.723	0.008
H(N11)	0.508	0.772	0.120
H(N11)	0.585	0.952	0.187
H(N11)	0.584	0.913	0.018

TABLE 2.6

Final anisotropic temperature factors (\AA^2) for non-hydrogen atoms.

ATOM	$U_{ij} \times 10^3$					
	U_{11}	U_{22}	U_{33}	U_{12}	U_{13}	U_{23}
O(1)	52(8)	41(8)	26(6)	7(6)	2(6)	5(5)
O(2)	88(11)	32(12)	52(9)	-1(7)	-4(8)	-6(6)
N(1)	67(11)	68(14)	27(8)	-13(9)	8(8)	-12(8)
C(1)	34(12)	44(16)	36(11)	0(9)	-6(8)	-8(8)
C(2)	94(19)	36(14)	40(12)	-3(11)	19(12)	10(8)
C(3)	32(12)	70(16)	74(14)	24(11)	15(11)	7(11)
C(4)	91(20)	101(22)	76(16)	13(18)	30(15)	-5(16)
C(5)	96(21)	109(26)	122(23)	-31(19)	-26(18)	32(20)
C(6)	48(17)	241(52)	139(26)	-21(23)	7(17)	87(29)
O(11)	51(8)	57(11)	21(6)	-2(7)	-6(6)	9(5)
O(12)	77(11)	50(12)	41(8)	9(7)	-5(7)	9(6)
N(11)	46(10)	44(9)	19(7)	6(7)	5(6)	0(6)
C(11)	41(13)	34(17)	47(12)	-4(9)	18(10)	8(8)
C(12)	66(14)	35(13)	39(10)	-8(10)	8(10)	3(8)
C(13)	26(11)	49(13)	59(12)	-15(9)	9(9)	9(9)
C(14)	114(23)	75(19)	51(13)	20(16)	30(14)	30(12)
C(15)	101(20)	80(20)	90(18)	20(17)	3(16)	-13(16)
C(16)	67(18)	135(29)	113(22)	-2(19)	14(16)	-32(20)

Errors in parentheses are estimated standard deviations.

TABLE 2.7 Bond lengths and angles in L-leucine.

(a) Intramolecular bond distances.

O(1) - C(1)	1.26(3) Å	O(11) - C(11)	1.27(3) Å
O(2) - C(1)	1.23(3)	O(12) - C(11)	1.25(4)
C(1) - C(2)	1.61(3)	C(11) - C(12)	1.57(3)
C(2) - N(1)	1.50(4)	C(12) - N(11)	1.53(3)
C(2) - C(3)	1.44(3)	C(12) - C(13)	1.50(3)
C(3) - C(4)	1.54(4)	C(13) - C(14)	1.54(4)
C(4) - C(5)	1.52(5)	C(14) - C(15)	1.44(4)
C(4) - C(6)	1.64(4)	C(14) - C(16)	1.68(4)

(b) Intramolecular bond angles.

O(1) - C(1) - O(2)	130(2)°	O(11) - C(11) - O(12)	128(2)°
O(1) - C(1) - C(2)	114(2)	O(11) - C(11) - C(12)	114(2)
O(2) - C(1) - C(2)	116(2)	O(12) - C(11) - C(12)	118(2)
C(1) - C(2) - N(1)	107(2)	C(11) - C(12) - N(11)	109(2)
C(1) - C(2) - C(3)	114(2)	C(11) - C(12) - C(13)	111(2)
N(1) - C(2) - C(3)	108(2)	N(11) - C(12) - C(13)	108(2)
C(2) - C(3) - C(4)	114(2)	C(12) - C(13) - C(14)	113(2)
C(3) - C(4) - C(5)	115(2)	C(13) - C(14) - C(15)	116(2)
C(3) - C(4) - C(6)	113(2)	C(13) - C(14) - C(16)	106(2)
C(5) - C(4) - C(6)	112(2)	C(15) - C(14) - C(16)	107(2)

Errors in parentheses are estimated standard deviations.

Fig. 2.2 Projection of structure down the b-axis

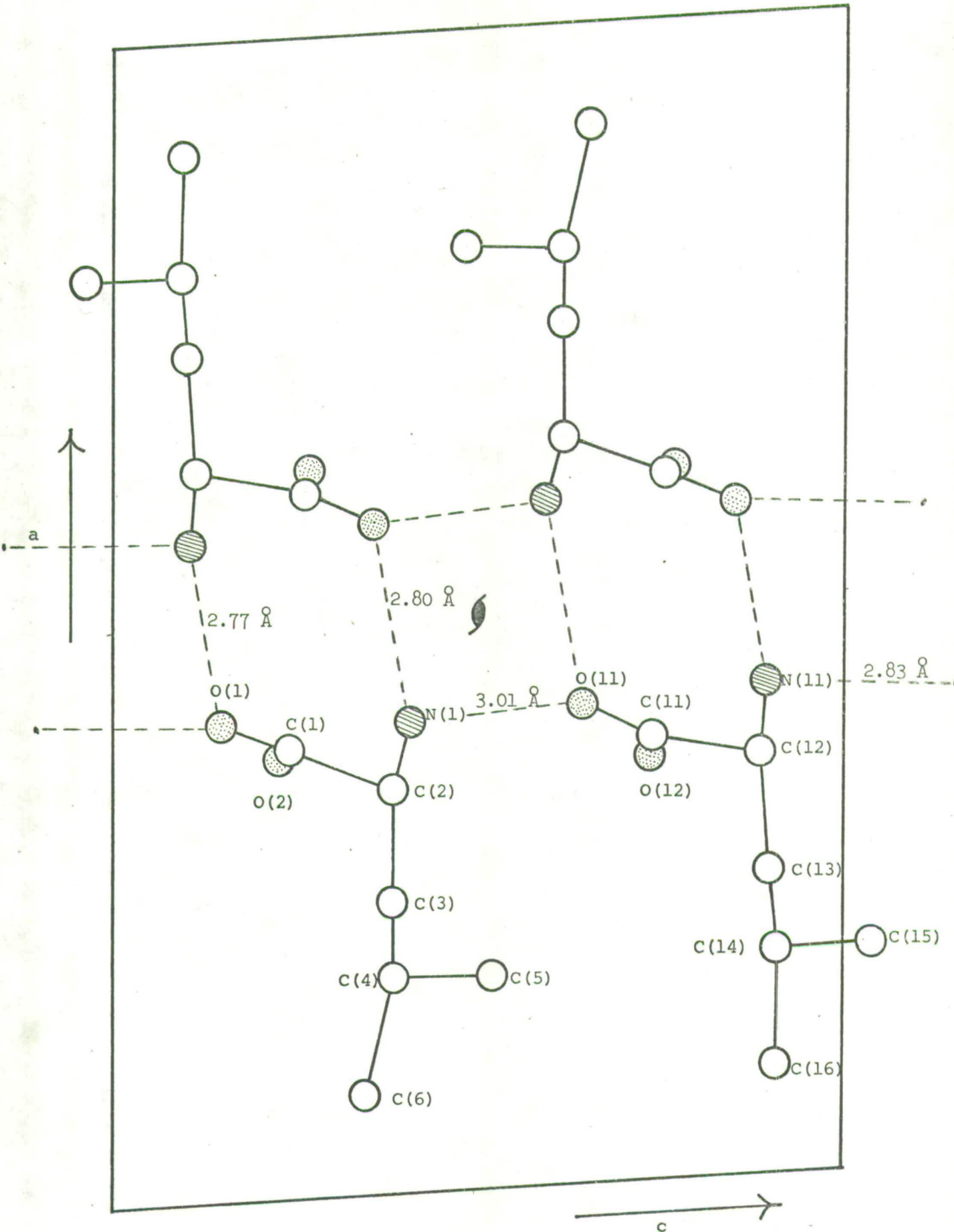


TABLE 2.8

Conformational angles in L-leucine.

O(1) - C(1) - C(2) - N(1)	-37.0°
O(2) - C(1) - C(2) - N(1)	147.9
O(1) - C(1) - C(2) - C(3)	82.0
O(2) - C(1) - C(2) - C(3)	-93.1
C(1) - C(2) - C(3) - C(4)	72.9
N(1) - C(2) - C(3) - C(4)	-169.0
C(2) - C(3) - C(4) - C(5)	64.2
C(2) - C(3) - C(4) - C(6)	-166.5
O(11) - C(11) - C(12) - N(11)	-27.5
O(12) - C(11) - C(12) - N(11)	152.8
O(11) - C(11) - C(12) - C(13)	91.2
O(12) - C(11) - C(12) - C(13)	-88.5
C(11) - C(12) - C(13) - C(14)	67.8
N(11) - C(12) - C(13) - C(14)	-172.6
C(12) - C(13) - C(14) - C(15)	68.8
C(12) - C(13) - C(14) - C(16)	-172.1

Note: A conformation angle is defined by looking along the bond from the second to the third named atom, a clockwise rotation of the front atom making a positive angle.

the two groups of atoms O(1), O(2), C(1), C(2) and O(11), O(12), C(11), C(12) are given by:

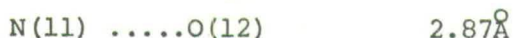
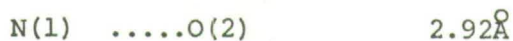
$$11.79x + 2.55y - 3.05z = 4.46$$

$$13.98x + 1.21y + 2.92z = 9.99$$

and N(1) and N(11) lie 0.99\AA and 0.66\AA out of these planes respectively.

The molecules are held together in the lattice by inter-molecular hydrogen bonds. Every nitrogen atom has 3 hydrogen atoms attached to it, and each of these is involved in a hydrogen bond to an oxygen atom of an adjacent molecule. As a result, every O(1) and O(11) atom is involved in 2 hydrogen bonds, one which runs approximately parallel to the c-axis, and the other which is approximately parallel to the a-axis.

Fig. 2.2 shows these bonds in projection down the b-axis, together with their corresponding lengths in angstroms. In addition, all nitrogen atoms hydrogen bond to oxygen atoms of molecules lying one unit of translation away and parallel to the b-axis. These two bond lengths are:

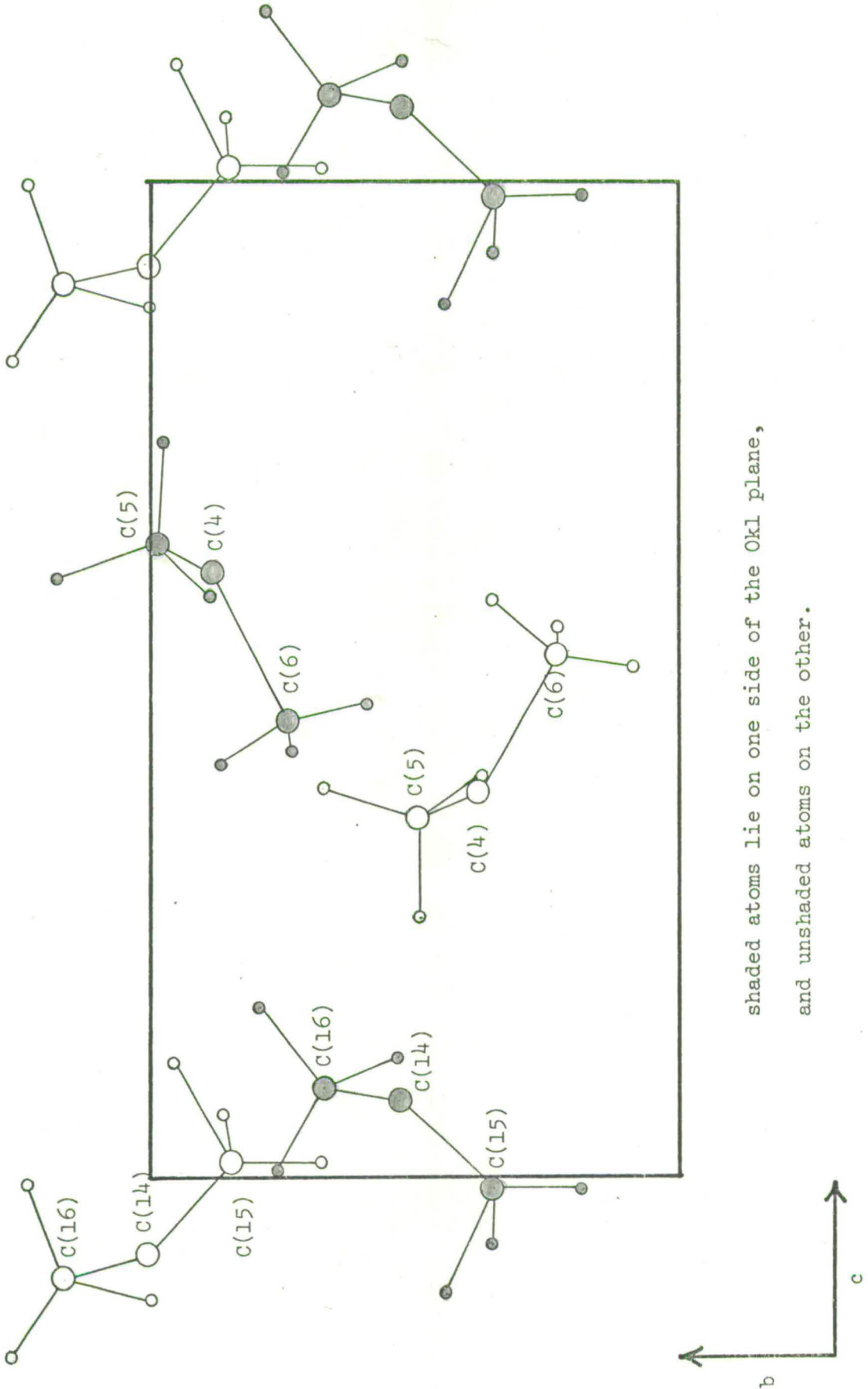


Thus at the carboxyl end of the molecules, the structure is held together by a 3-dimensional array of hydrogen bonds, all of whose lengths are very satisfactory.

At the other ends of the molecules, the hydrocarbon ends, only Van der Waal's ^{bonding} is possible, and it is clearly this lack of possible bonding which causes crystals of the compound to form such very thin plates, i.e. the crystals do not develop readily along the a-axis.

Fig. 2.3 is an a-axis projection to show how the terminal methyl groups from one cell pack against those from an adjacent cell. This does not seem to be an ideal way of packing as there are spaces left unfilled, and some apparently close contacts elsewhere. C(15), for example, appears

Fig.2.3 Projection of structure down the a-axis showing the packing of terminal methyl groups from adjacent unit cells.



to be close to C(16) in the adjacent cell, however, a further look at Fig.2.2 reveals that they are in fact well spaced. It is most probably the demands of packing and hydrogen bonding at the carboxyl end of molecules which is causing these slight imperfections in packing at the hydrocarbon ends.

There are 5 intermolecular close contacts less than 3.8 Å within the molecule. These are:-

N(1)	C(11)*	3.62 Å
N(1)	N(11)*	3.68
C(1)	N(11)*	3.72
O(2)	C(2)**	3.46
C(2)	O(12)***	3.51

where * = other unique molecule within the unit cell which lies approximately parallel to the a-axis,

** = adjacent molecule approximately parallel to the -c-axis,

and *** = adjacent molecule approximately parallel to the +c-axis.

CHAPTER 3

THE CRYSTAL STRUCTURE OF DL-LEUCINE

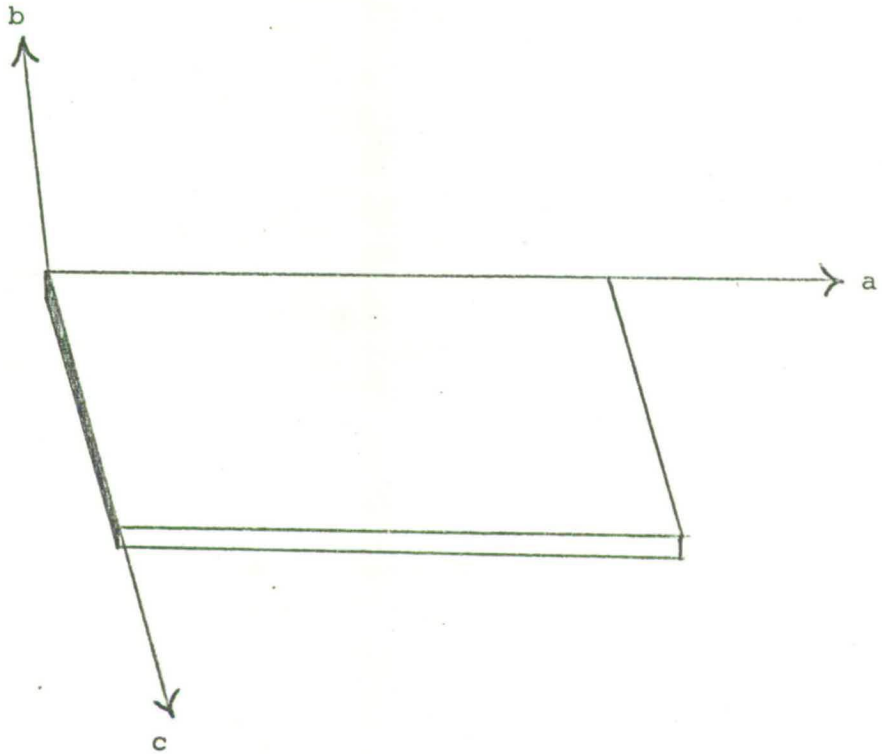
3.1 Crystal Growth

Like the previous compound, L-Leucine, this amino-acid was obtained as a commercial sample from BDH and then recrystallised by isothermal distillation methods using ethanol and distilled water as the two solvents. Crystals formed as very thin clear plates which curled up very easily if shaping was attempted. Thus only crystals requiring no cutting could be used. A major problem in growing these crystals appeared to be that it was impossible to separate out a single crystal, instead all crystals appeared on X-ray analysis to exist as twins. Eventually, it was decided to proceed with one of these twinned crystals, and for the sake of collecting reflection data, to ignore one set of Weissenberg festoons where appropriate.

3.2 Preliminary X-ray work

A crystal of dimensions 0.0125 x 0.225 x 0.305 mms. was selected and mounted on a thin glass capillary tube. It was then mounted on a Pye Unicam Weissenberg Camera. The radiation used throughout was Cu K_α , of wavelength 1.5418 Å. Oscillation and Weissenberg photographs of the layers $0k\ell$, $1k\ell$, $hk0$ and hkl were taken, and approximate cell dimensions derived. β^* is the most difficult cell dimension to obtain from these photographs, and an error in the initial value was only discovered when difficulties occurred in the refinement. (It is corrected below). Fig.3.1 shows the morphology of a typical crystal together with the associated crystal axes.

Fig. 3.1 Typical crystal morphology of DL-leucine, with its associated crystal axes



3.3 Cell dimensions and Space-group

For accurate cell dimensions, very high angle diffraction data could not be recorded. The best available data in the range $\theta = 5^\circ$ to 75° , was used to determine values for all the reciprocal cell dimensions, and then the values extrapolated to $\theta = 90^\circ$.

By this method, the following cell dimensions were obtained (standard deviations being quoted as errors):-

$a^* = 0.3061$ r.l.u.	$a = 5.430(.04)$ Å
$b^* = 0.1112$ r.l.u.	$b = 13.966(.04)$ Å
$c^* = 0.3203$ r.l.u.	$c = 5.166(.04)$ Å
$\alpha^* = 84.32^\circ$	$\alpha = 96.7^\circ(0.2)$
$\beta^* = 110.93^\circ$	$\beta = 68.8^\circ(0.2)$
$\gamma^* = 88.40^\circ$	$\gamma = 93.9^\circ(0.2)$

The density of the crystals was measured by the flotation method using commercial alcohol and carbon tetrachloride as the two liquids. From this $\rho = 1.21$ gm cm⁻³. The cell volume, V, is given by:

$$V = abc\{1 - \cos^2\alpha - \cos^2\beta - \cos^2\gamma + 2\cos\alpha \cdot \cos\beta \cdot \cos\gamma\}^{\frac{1}{2}}$$

$$= 362.5 \text{ Å}^3$$

From the observed density and cell volume, the number of molecules in the unit cell is given by:-

$$Z = \frac{V \times \rho \times N_0}{F \times 10^{24}} = 2.03 \approx 2 \quad \text{where } N_0 = \text{Avogadro's No.}$$

$F = \text{Formula Weight}$

To decide, finally, whether the crystal belonged to space-group $P1$ or $\overline{P1}$ also proved interesting. In the original paper on the compound(37), it was stated that the crystals showed piezo-electric properties, thus indicating that the space-group was acentric, i.e. $P1$. On endeavouring to repeat this experiment, no such piezo-electric effect was observed; however, a negative result is not conclusive. It was shown later by looking at the intensity statistics (Table 3.1) that in fact the cell was centric as a first approximation, but could only be fixed definitely at the refinement stage. Thus space-group $\overline{P1}$ was used to begin with.

3.4 Collection of 3-dimensional data

3-Dimensional reflection data ^{was} ~~was~~ collected using a Pye Unicam Weissenberg camera. A crystal was mounted first about the c-axis when layers 0-3 inclusive were collected, and then about the a-axis, again layers 0-3 being recorded. Data was collected using multi-film packs of Kodak Kodirex film, and exposure times ranged from 4 to 96 hours. The films were then scanned by the SAAB scanner (see Appendix I). The tape files were then processed by a sequence of computer programs. MAPFILM sorts through the intensities and organises them into spots. Each spot is given a serial number and printed out with the co-ordinates of its centre, together with any necessary indications as to whether the spot had a distorted shape, or was too black to have been measured accurately by the scanner. These serialised spots are then printed out on a reconstructed map of the film so that suitable spots can be indexed for the next stage which is READFILM. This program takes these selected spots

TABLE 3.1

Statistical analysis of normalised structure factors to determine whether space-group is centric or not.

	Experimental	Theoretical	
		Centric	Acentric
Average E	0.828	0.798	0.886
Average E^2	1.00	1.00	1.00
Average $ E^2-1 $	0.917	0.968	0.736
Average $(E^2-1)^2$	1.61	2.00	1.00
Average $ E^2-1 ^3$	5.05	8.00	2.00

(up to 39) and uses them to calculate certain film parameters by least squares refinement. These parameters are XO and YO (origin of lattice), D (film diameter when mounted in the cylindrical camera), R (the distance traversed down the film before encountering a duplicate reflection), and T (the angle of distortion, if any, that the lattice is displaced from a lattice recorded from a perfectly set crystal). Having carried out the refinement, all possible spot positions are calculated, and a frame set up (of specified dimensions) around each point. The MAPFILM file is then searched, and all intensity readings within the frame are summed and listed as the integrated intensity for that reflection. Finally, the program writes all the intensity data onto file and prints out maps of a few selected spots in order that it can be checked that their shapes are acceptable.

When all films for a particular layer have been processed in this manner, the tape files are used as input for PACKSCALE which scales the data together, and prints out on paper, and cards, a final list of reflection intensities. The intensities were corrected for Lorentz and polarisation factors before being scaled together.

Using the above system, a set of cards was built up containing the data for all reflections with observed intensities. In order to be able to apply a statistical analysis to these intensities, reflections which were very weak or not observed at all were then added manually to the card deck. 953 reflections were used in the deck, 301 of which were classed as "less-thans", i.e. very weak.

3.5 Absorption Corrections

Even though the data collected for this compound was probably more accurate than for L-leucine, it was still thought unnecessary to apply any absorption corrections since there were no atoms present in the unit cell heavier than oxygen.

(Linear absorption coefficient = 6.2 cm^{-1}).

3.6 Trial Structure

A similar approach to that used for L-leucine was used for DL-leucine, but to begin with X-RAY system was made use of rather than NORM. A brief description of the various programs required is given in Appendix III.

After running DATRDN, normalised structure factors were calculated using NORMSF. E's are determined from the following relationship:-

$$|E_{hkl}| = \frac{|F_{hkl}| \times D}{\{P \times \sum F_j^2\}^{1/2}}$$

where D = F relative scale factor correction to ensure that the average value of $|E|^2 = 1.0$

F_j = the J^{th} scattering factor at the appropriate $\sin\theta/\gamma$ value for the reflection.

P = correction factor allowing for space-group symmetry.

These normalised structure factors were then input into MULTAN, the purpose and workings of which have already been described briefly in section 2.6. Table 3.2 lists the starting reflections produced by CONVERGE, and gives the phases of the two most promising sets found by FASTAN. Their figures of merit (see 2.6) are shown



TABLE 3.2

Starting reflections and phases for two sets as found by MULTAN

(i) Origin fixing reflections:

	<u>Reflection</u>			<u>Phases</u>	
				<u>Set 1</u>	<u>Set 2</u>
1	-12	0		0	0
0	7	3		0	0
2	-13	0		0	0

(ii) Other reflections in starting set:

	<u>Reflection</u>			<u>Phases</u>	
				<u>Set 1</u>	<u>Set 2</u>
2	-5	3		180	180
4	-2	-1		180	180
2	5	-3		180	180
0	6	0		0	180

N.B. Phases are in degrees

in Table 3.3. Using the second of these sets, a very plausible set of peaks was obtained from its E-map. By plotting these peaks on a model, and using it in conjunction with BONDLA which calculated the distances and angles between them, 7 peaks were assigned to atoms, and these are listed with their fractional co-ordinates in Table 3.4. The numbering system of atoms within the molecule is the same as for molecule A of L-leucine (see Fig. 2.1).

3.7 Refinement of structure

Having chosen the most suitable peaks and assigned them to specific atoms, a series of jobs was run using the X-RAY system. DATRDN absorbed the reflection data and cell dimensions. Scattering factors for C, N, O and H atoms were supplied automatically by the system using those calculated from Hartree-Fock wave functions(42). Using simply the atomic co-ordinates indicated by the E-map, a residual factor, R, of 0.56 was obtained.

The structure was then improved using FOURR which could be used to construct difference Fourier maps, which indicated appropriate atom shifts. By this means, the residual factor was reduced to 0.44.

At this stage the structure was thought to be well enough known to embark on a refinement by least squares methods using CRYLSQ. Since the space-group was centric, it was possible to refine all atomic parameters, temperature and scale factors at the same time. To begin with, each atom was allocated an individual isotropic temperature factor of $U = 0.038$ where

$$U = \frac{B}{8\pi^2}$$

B is the more common form of temperature factor and is defined as:-

$$\text{change in scattering power} = \exp\{-B \sin^2\theta/\lambda\}$$

TABLE 3.3

Figures of merit of the two starting sets of phases found by MULTAN

	<u>Set 1</u>	<u>Set 2</u>
ABS FOM =	1.2100	1.2679
PSI ZERO =	0.0	0.0
RESID =	23.93	19.76

TABLE 3.4

Fractional co-ordinates of atoms found from E-map

<u>ATOM</u>	x	y	z
O(1)	0.75	0.42	1.01
O(2)	0.75	0.42	0.69
N(1)	0.24	0.43	0.69
C(1)	0.57	0.40	0.88
C(2)	0.27	0.36	0.87
C(3)	0.18	0.27	0.76
C(4)	0.27	0.19	0.95

Full-matrix least squares was used throughout as the relatively small number of parameters to be refined meant that computer jobs were not very long. Using the above method, R was then reduced to 0.128. From this point, temperature factors were made anisotropic and the layer scale-factors were restricted to a constant ratio when R was further reduced to 0.115.

Finally, since it was hoped that this data would be more accurate than the visually measured data of L-leucine, a difference Fourier map was obtained using FOURR in order that hydrogen atoms might be found. Using a combination of this map, a model of the structure to indicate possible sites for these atoms, and BOND (Dr. R.O. Gould - see section 2.7) hydrogen atoms were located on all atoms where expected, except for C(6). However, these were not included in the final structure factor listing given in Appendix III.

Mention was made in section 3.3 of the fact that only the intensity statistics indicated that the structure was centric rather than acentric. In order to test this, the structure was assumed acentric, and some of the atoms, in particular those related by symmetry to C(4), C(5) and C(6) were moved off their calculated positions. Least squares refinement of these atoms shifted these positions very close to the original ones, which strongly suggested that the structure is indeed centric.

3.8 Description of Structure

The final list of atomic parameters, including the 10 hydrogen atoms, is given in Table 3.5, whilst Table 3.6 lists the anisotropic temperature factors for the non-hydrogen atoms. The intramolecular

TABLE 3.5

Final positional parameters of an L-leucine molecule in DL-leucine.

Errors in parentheses are estimated standard deviations.

<u>ATOM</u>	<u>x</u>	<u>y</u>	<u>z</u>
O(1)	0.7342(10)	0.4132(4)	0.6751(12)
O(2)	0.5884(10)	0.3878(4)	0.1224(15)
N(1)	0.2318(11)	0.4297(4)	0.6830(14)
C(1)	0.5527(15)	0.3908(5)	0.8964(22)
C(2)	0.2789(14)	0.3677(5)	0.8774(17)
C(3)	0.2623(17)	0.2648(5)	0.7595(19)
C(4)	0.2556(19)	0.1898(6)	0.9609(22)
C(5)	0.9793(22)	0.1870(7)	0.1853(24)
C(6)	0.3200(25)	0.0899(8)	0.7987(28)
H(N1)	0.334	0.492	0.684
H(N1)	0.039	0.443	0.749
H(N1)	0.286	0.394	0.492
H(C2)	0.139	0.379	0.067
H(C3)	0.100	0.255	0.710
H(C3)	0.417	0.253	0.583
H(C4)	0.075	0.187	0.106
H(C5)	0.046	0.132	0.262
H(C5)	0.035	0.242	0.333
H(C5)	0.155	0.191	0.097

TABLE 3.6

Anisotropic temperature factors (\AA^2) for non-hydrogen atoms.

$$U_{ij} \times 10^3$$

<u>ATOM</u>	U_{11}	U_{22}	U_{33}	U_{12}	U_{13}	U_{23}
O(1)	20(3)	43(3)	32(4)	-5(2)	-21(3)	7(3)
O(2)	20(3)	35(3)	30(5)	-4(2)	-15(3)	3(3)
N(1)	20(3)	29(3)	26(4)	1(3)	-9(3)	7(3)
C(1)	21(4)	16(4)	38(7)	0(3)	3(4)	3(4)
C(2)	17(4)	26(4)	32(5)	-2(3)	-19(3)	1(4)
C(3)	44(5)	27(4)	38(6)	-1(3)	-18(4)	0(4)
C(4)	52(6)	34(5)	65(7)	0(4)	-16(5)	9(5)
C(5)	66(7)	61(6)	67(8)	0(5)	0(6)	26(5)
C(6)	93(10)	50(6)	94(10)	9(6)	-20(8)	4(6)

Errors in parentheses are estimated standard deviations.

bond distances and angles are given in Table 3.7, and, as for L-leucine, there are no significant differences from the dimensions listed in Table 1.5. As was to be hoped, the standard deviations in co-ordinates, and hence in intramolecular geometry, are much better for DL-leucine due to the greater accuracy of the intensity data. A projection of the structure is shown in Fig. 3.2, looking down the c-axis.

The conformation angles for an L-molecule are given in Table 3.8 and these closely resemble the corresponding angles in L-leucine (see Table 2.8). Projections of all 3 L-molecules are shown in Fig. 3.3 for comparison. The angles around bond C(2) - C(3) correspond to an almost fully staggered conformation, while those around C(3) - C(4) lie approximately half-way between staggered and eclipsed. The equation of the plane through the carboxyl group and C(2) is given by:

$$-1.40x + 13.52y - 0.17z = 4.41$$

with N(1) lying 0.96 \AA out of this plane.

As in L-leucine, the molecule exists as a zwitterion with its nitrogen atom bonded to 3 hydrogen atoms. Each of these hydrogen atoms is involved in a hydrogen bond to adjacent molecules. N(1) is bonded to O(2) of the centro-symmetrically related molecule (2.99 \AA), to O(2) of the adjacent molecule along the a-axis (2.71 \AA), and to O(1) of the adjacent molecule along the c-axis (2.86 \AA). This arrangement of hydrogen bonding, shown in Fig. 3.2, holds the molecules together at the carboxyl ends, but at the hydrocarbon ends only weak Van der Waal's bonding is possible, which explains why the crystals cleave so readily into platelets at right angles to b^* .

TABLE 3.7 Bond lengths and angles in DL-leucine

(a) Intramolecular bond distances

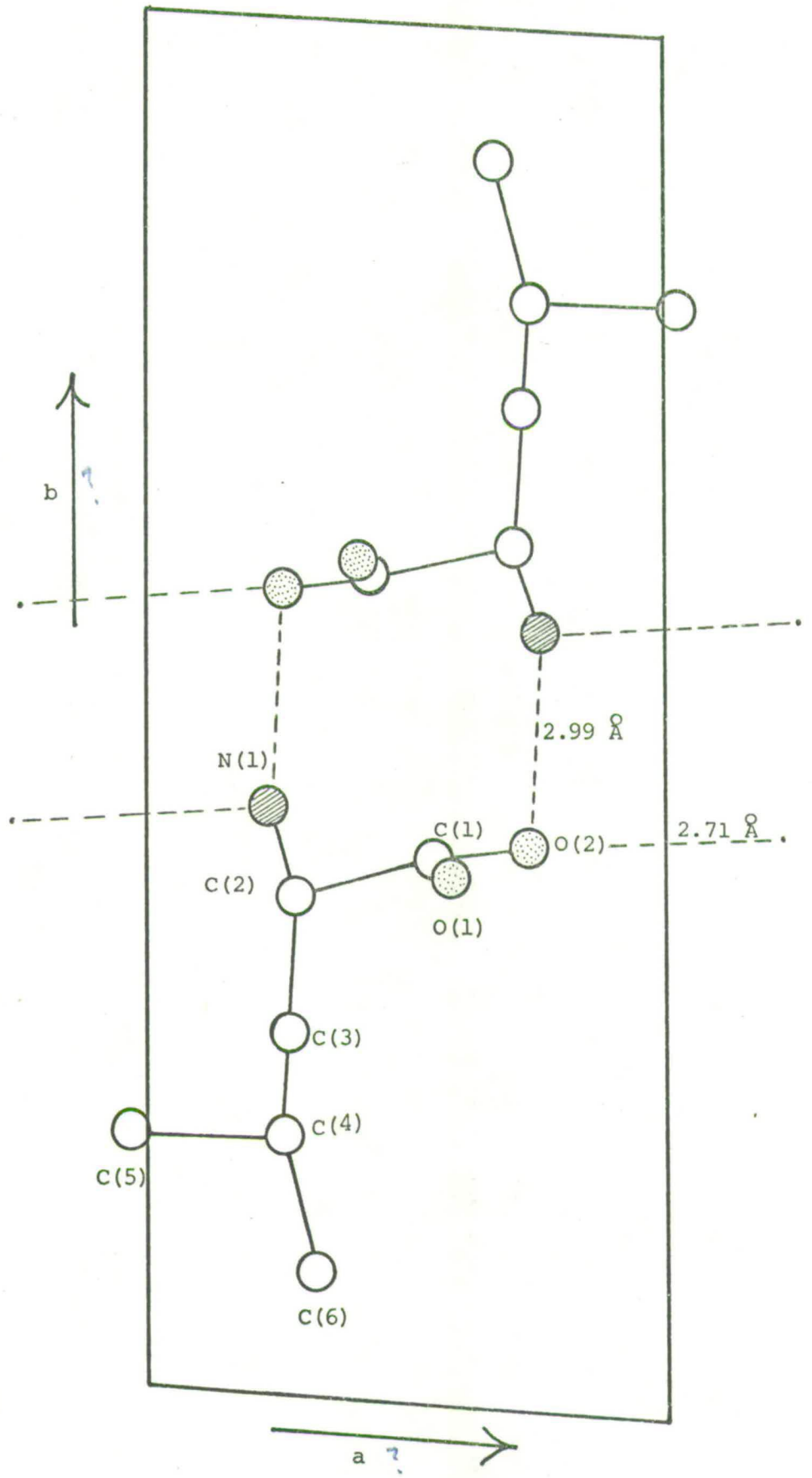
O(1) - C(1)	1.266(10) Å	O(2) - C(1)	1.256(15) Å
C(1) - C(2)	1.535(12)	C(2) - N(1)	1.498(12)
C(2) - C(3)	1.503(10)	C(3) - C(4)	1.550(15)
C(4) - C(5)	1.531(13)	C(4) - C(6)	1.534(14)

(b) Intramolecular bond angles

O(1) - C(1) - O(2)	123.2(8)°
O(1) - C(1) - C(2)	116.3(1.0)
O(2) - C(1) - C(2)	120.5(1.0)
C(1) - C(2) - N(1)	110.4(6)
C(1) - C(2) - C(3)	110.3(6)
N(1) - C(2) - C(3)	106.7(7)
C(2) - C(3) - C(4)	113.7(8)
C(3) - C(4) - C(5)	108.7(9)
C(3) - C(4) - C(6)	109.9(9)
C(5) - C(4) - C(6)	109.8(8)

Errors in parentheses are estimated standard deviations.

Fig. 3.2 Projection of structure down the c-axis



○ = carbon

● = oxygen

◐ = nitrogen

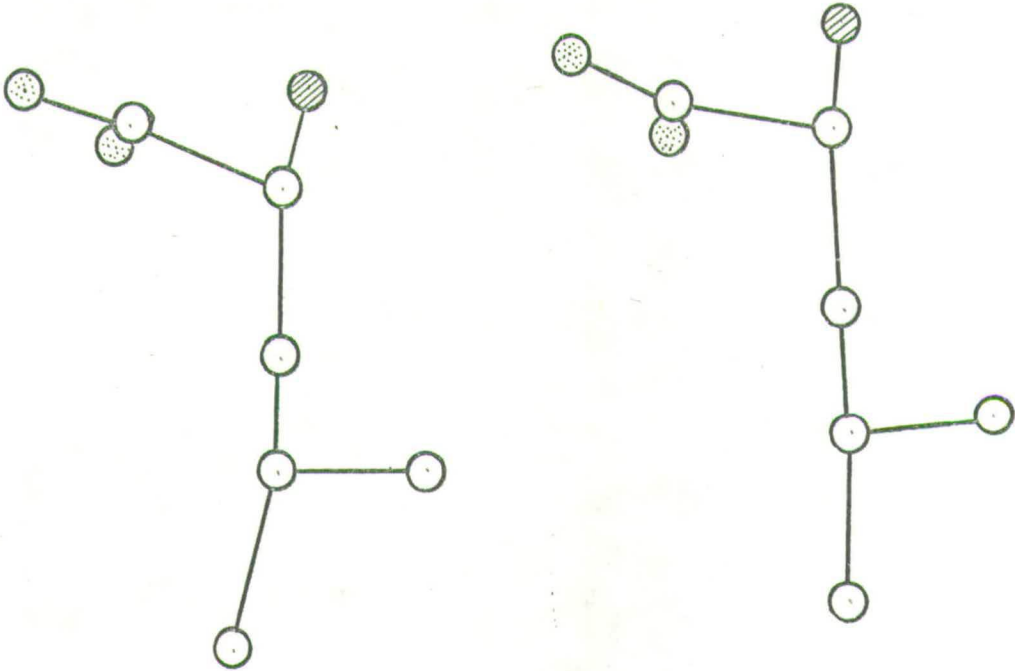
TABLE 3.8

Conformation angles of the L-molecule in DL-leucine

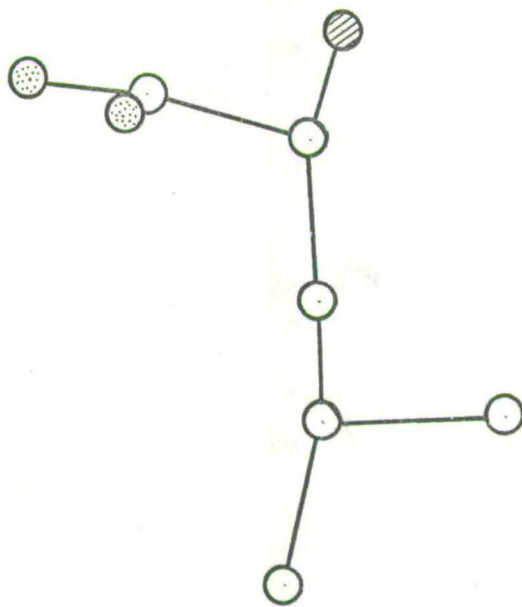
O(1) - C(1) - C(2) - N(1)	-34.8°
O(2) - C(1) - C(2) - N(1)	144.6
O(1) - C(1) - C(2) - C(3)	82.8
O(2) - C(1) - C(2) - C(3)	-97.7
C(1) - C(2) - C(3) - C(4)	70.6
N(1) - C(2) - C(3) - C(4)	-169.5
C(2) - C(3) - C(4) - C(5)	76.2
C(2) - C(3) - C(4) - C(6)	-163.6

Note: A conformation angle is defined by looking along the bond from the second to the third named atom, a clockwise rotation of the front atom making a positive angle.

Fig. 3.3 Comparison of the projections of the 3 L-molecules as found in the crystal structures.



L-LEUCINE



DL-LEUCINE

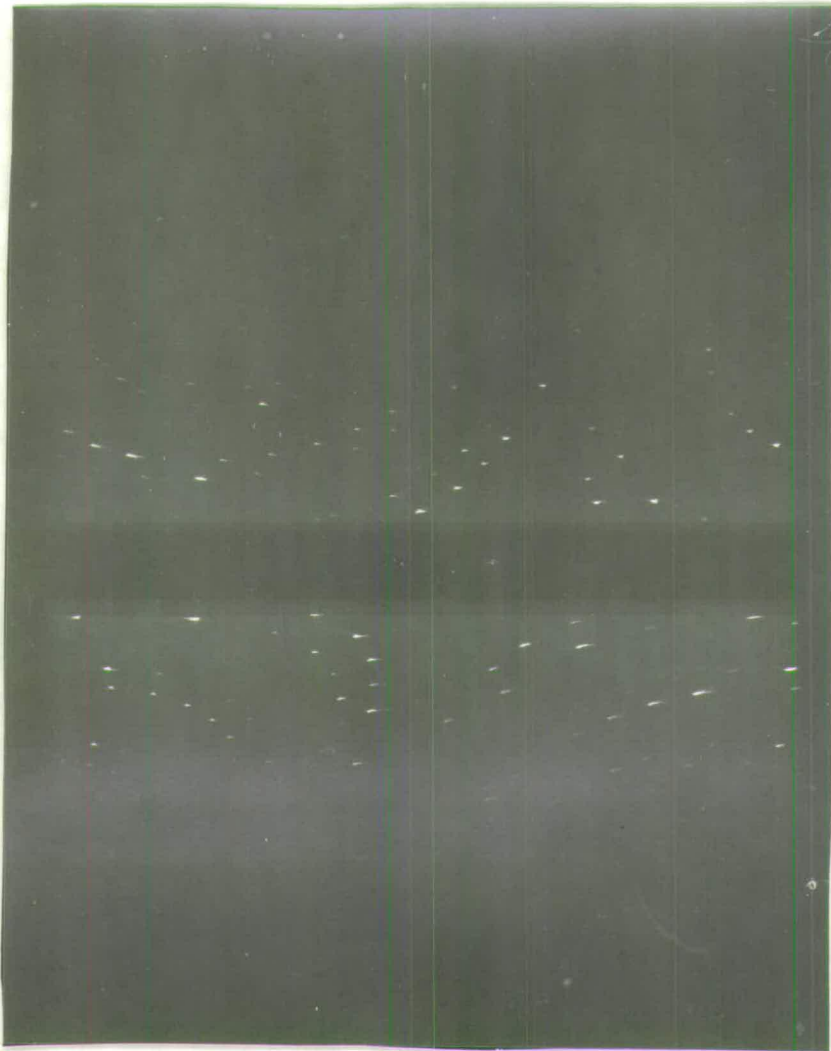
The only intermolecular close contacts in the crystal (i.e. less than 3.6 Å) are from N(1) to N(1) and C(1) of the symmetry related molecule. These distances are 3.47 Å and 3.54 Å respectively.

3.9 Conclusions

This crystal structure showed two features worthy of mention, neither of which were evident in L-leucine. First, the crystal belongs to a triclinic space-group, and as yet all other amino-acids have either been monoclinic or orthorhombic. The original work done on this structure(37) indicated a triclinic space-group, but suggested it was $P1$, and not $P\bar{1}$ as has been found. Their evidence for this was that crystals showed piezo-electric properties. Even though the intensity statistics indicated some uncertainty in the space-group, it is difficult to see how they succeeded in obtaining a positive result for their crystals.

The other, slightly annoying, feature of this compound, is that it will not form single crystals, but instead forms twinned crystals that cannot be separated. As a result, upper-layer Weissenberg photographs taken up the c-axis showed two sets of festoons. An example of one of these photographs is shown in Fig. 3.4. These festoons did not appear in the zero-layer, however, nor in any of the photographs taken of the crystal mounted about the a-axis. In order to determine the nature of the twinning, a reciprocal lattice was constructed for the hkl planes where both twins appeared. This revealed that one twin was related to the other by a rotation of 180° about the b^* -axis, in other words the crystal platelets stacked together with some of the plates rotated by 180° about the axis normal to the plates.

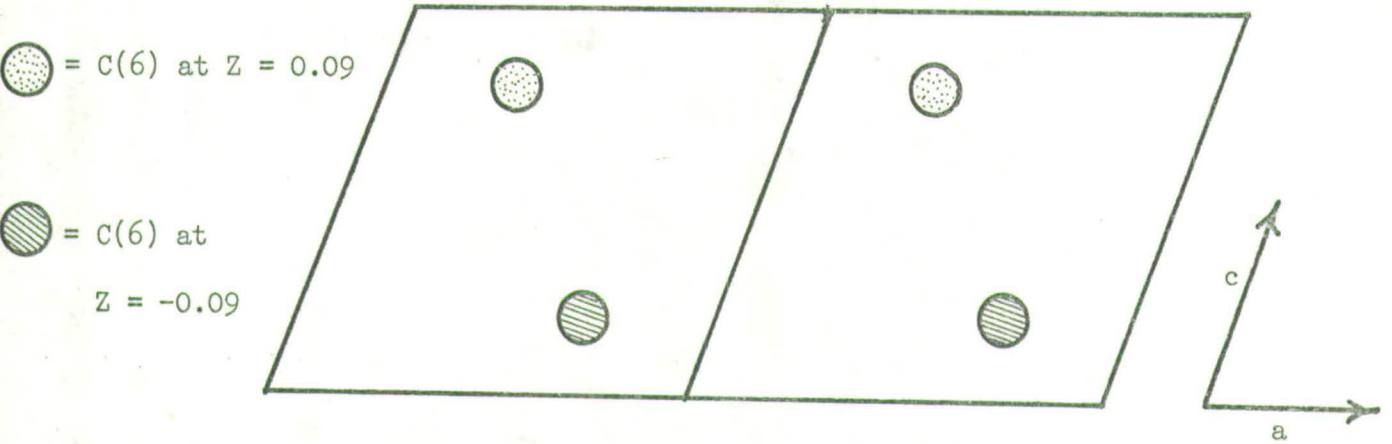
Fig. 3.4 Example of first-layer Weissenberg photograph
taken up the c-axis



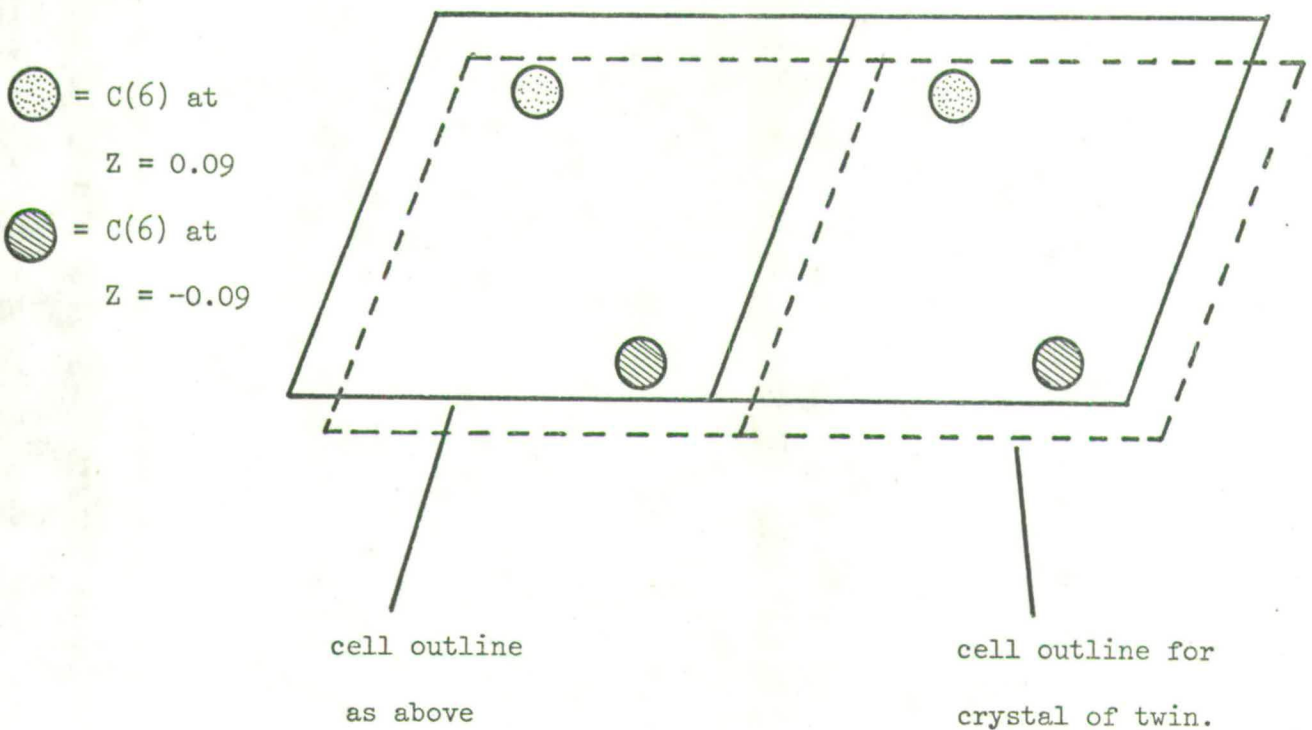
The fact that the compound forms twins so readily indicates that the packing of two molecules across the ac-plane must be energetically very similar for two normal cells, and two cells from different twins. The only atoms which affect the packing at this point are C(6) and its associated hydrogen atoms. In the normal case, C(6) will fit neatly between the four C(6) atoms which are found across the ac-plane; for the twin, a shift of $(\frac{1}{2}, 0, \frac{1}{2})$ by one cell on the other gives an almost equally favourable form of packing. It is this possibility of one crystal face being able to slide easily over another that makes twinning so common in this structure. Fig. 3.5 illustrates a possible arrangement of this packing.

Fig. 3.5 Normal and faulty packing across the h0l plane.

(a) Normal stacking



(b) Faulty stacking - the displacement of the cell edges of the two twins is not known, but an arrangement such as follows would allow good packing of the methyl groups.



APPENDIX I

THE SAAB MARK II AUTOMATIC

FILM SCANNER

INTRODUCTION

Despite the tremendous advances made in automatic diffractometers, data collection by film methods is still very common. Combined with an automatic film scanner, the latter method makes possible fast and economic data collection for single crystal work. This becomes more important as the complexity of the structures investigated increases. Moreover, an automatic film scanner can serve a large number of cameras, whereas a diffractometer is tied to one crystal for an appreciable length of time.

A prototype scanner was built and described by Abrahamsson in 1966 (43). The principles of its operation were identical with those of the scanner in this laboratory, however, because the computer linked to the scanner was not fast enough to collect all the data transmitted, only data above the local background was stored. For Weissenberg films, this was taken as the mean transmission of a complete track. In order to examine very weak reflections, the cut-off value had to be set as low as possible, and as a result, great care had to be taken not to put any extraneous marks, such as fingerprints, on the film as these would be measured. It was shown that repeated measurements of the same film, even after several days interval gave a reproducibility of spot intensities of around 3%. Examination of a multi-film pack gave constant film factors, within the linear range of the scanner, except for very weak reflections which tended to be underestimated. On a complete structural analysis of dimethyltrithiabicycloheptane, the data was refined down to $R = 4.4\%$.

A similar scanner to that of Abrahamsson was described by Xuong in 1969 (44). He made certain modifications which improved the precision of the film position and the optical density measurement. The instrument was connected to a third generation computer with a magnetic disk drive large enough to store the image of an entire film. The rotating drum which holds the film was larger, 5" in diameter, and contained 2 rectangular apertures on opposite sides of the drum, one of which was used as a reference. The advantages claimed were first, that the film was less distorted which meant that spot positions were known with greater accuracy, and second, measurement of the incident beam intensity once every revolution overcame the possible error in optical density measurements due to instability of the source. Using this scanner, they found that spot positions were accurate to 100 μm , and that intensities were reproducible to within $\pm 1\%$. By application of a correction term, it was also found that they could also increase the useful density range from 1.0 up to 2.2. As further tests of accuracy, all spots on one film were measured twice, and this gave $R = 3\%$; comparing intensities on one film of symmetry related spots gave $R = 6\%$.

An evaluation of an automatic film scanner similar to that described by Abrahamsson and Xuong was carried out by Nockolds and Kretsinger (45). The incident beam in this case was circular in cross-section with possible diameters 50, 100 or 200 μm , but satisfactory results were still obtained, even though a film image consisted of a square array of circles. All their work was concerned with precession photographs of protein crystals, and they defined one axis by positioning it parallel ($\pm 15'$) to the direction of scanning.

Spots on precession films being of approximately the same size and shape, intensities were summed within a rectangle of constant size for any particular film. The background was determined by an examination of the readings immediately surrounding this box. Integrated intensities were then defined as:-

$$I = \Sigma D - \Delta x \Delta y B$$

where ΣD is the sum of the intensities within a box of size $\Delta x \Delta y$, and B is the background.

They found that boxes for very weak reflections appeared to be too large, but for strong reflections, if too small a box is used, not only are some intensity readings not included in ΣD , but they are used in the background calculation. Thus their programmes had to be flexible enough to allow the box size to be changed easily. Using the aperture of 200 μm diameter, they found that spot intensities were reproducible to $R = 13\%$. In coping with split spots, it was found satisfactory ^{it} simple to choose a box large enough to include both parts. The maximum range of optical density which could be used accurately was taken as 2.3. Within these limits, spot intensities were reproducible to 1%.

Another investigation into the accuracy of film scanners was done by Werner (46). He used a SAAB model, similar to the one in this laboratory, which used a light beam of rectangular cross-section 90 x 60 μm . Data was stored on magnetic tape mounted on a third generation computer. Intensities of about one hundred thousand reflections from horse liver alcohol dehydrogenase and 3 isomorphous heavy atom derivatives were measured, and accuracy of these measurements

was tested for in various ways. As a check for random errors, symmetry related spots were compared, when it was found that any individual measurement varied by up to 4% from the average. For very weak reflections, this value increased to about 12%. Compared to similar measurements using a Joyce-Loebl microdensitometer, these figures are about $1\frac{1}{2}$ times greater. An examination of film factors between films showed that when I_1/I_2 was plotted against I_1 (the intensity on the stronger film), there was a small but significant fall as I_1 increased. The reason for this was not fully understood. Comparing structure factor sets obtained from different film sets, results were reproducible to within 3.4% on average. It was concluded that because of problems such as streaks, spot shape variance, and $\alpha_1\alpha_2$ splitting, film scanners were of more use in processing precession rather than Weissenberg films.

In order to collect data for 2,5-dimethyl-2,5-endo-thio-1,4-dithiane, O'Connell (47) made use of a film scanner. To obtain an idea of its accuracy, film factors for all reflections on adjacent films were calculated, and the film factor distribution was plotted against intensity. It was found that there were some systematic errors in low intensity terms due to the method used for the integration of intensities. These distributions were also found to be useful in finding the upper limit of the linear range of the instrument.

II Description of film scanner

Working principle: Fig. I shows a picture of the scanner, and Fig. II shows the working principle of the equipment in a block diagram. The film, which carries the information as a pattern of transparency variations, is placed in a special film holder. A light beam, the cross-section and stability of which are strictly controlled, illuminates a spot of the film. By a feeder mechanism the film is rotated and translated to allow the light beam to scan the film in parallel tracks. The light which penetrates the film is then converted by a photomultiplier into a DC voltage which is proportional to the film transmission. This voltage, duly amplified, produces the data output from the scanner referred to a system of orthogonal co-ordinates. The co-ordinate pattern forms rectangles of $60 \times 45 \mu\text{m}$ or $60 \times 90 \mu\text{m}$. The scanning times for a film measuring $100 \times 135 \text{ mins.}$ are 15 and 7.5 mins. respectively.

To refer the light spot position to the film co-ordinate system, the feeder mechanism features "position pulse generators" giving 3 kinds of signals:-

- (i) "Stand by" signals indicating that the scanning head is safely outside the film area,
- (ii) 1 pulse at the beginning of each track,
- (iii) 1 pulse for every co-ordinate unit along each track.

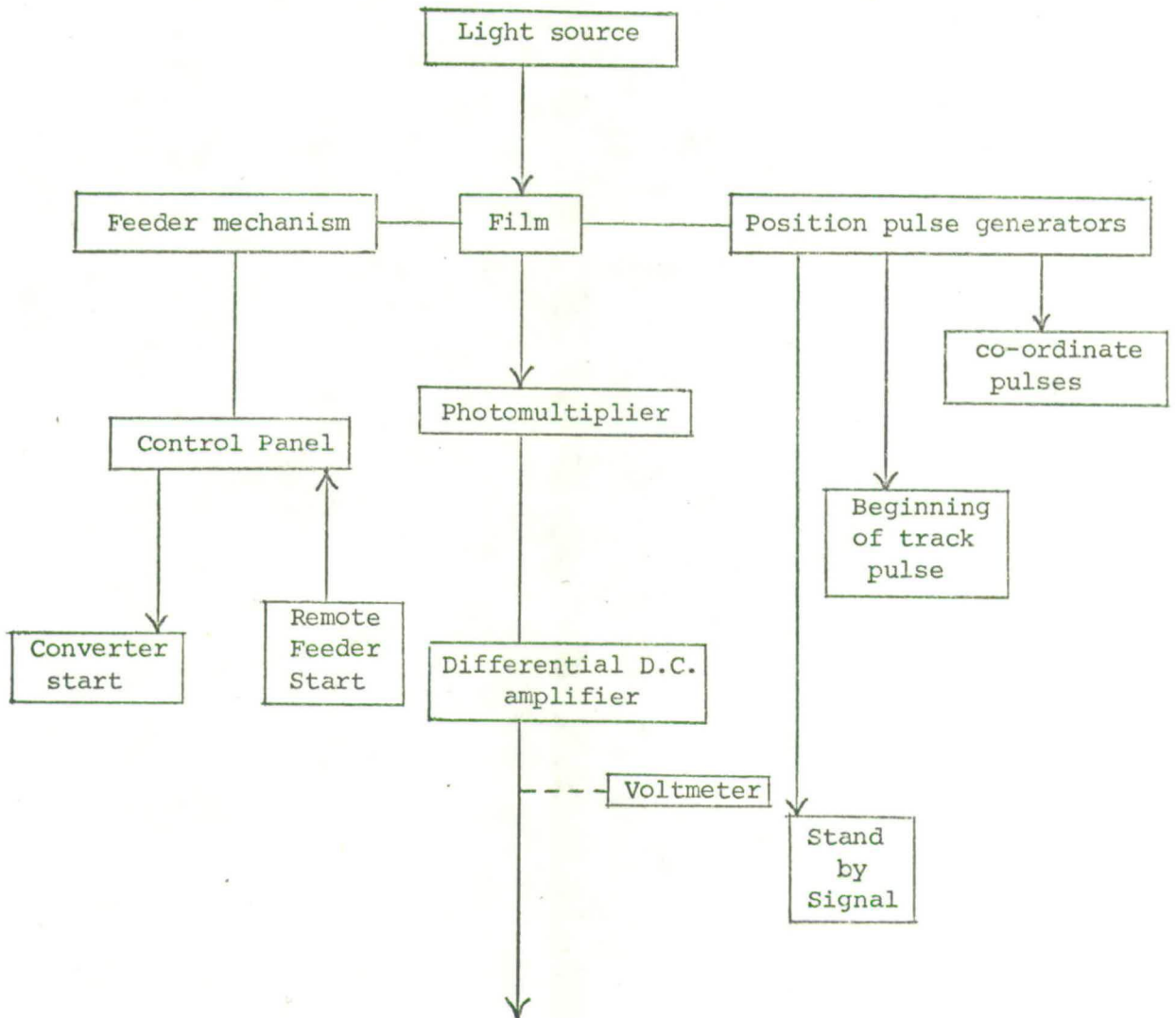
The control buttons of the feeder mechanism are placed in a control panel on the front of the scanner. Starting and stopping of the scanner can either be by buttons on the control panel, or by remote-control (e.g. if the scanner is linked directly to a digital computer). In fact the former method is used.

Fig. I

The SAAB Mark II film scanner



Fig. II Block diagram of the working principle of the
film scanner



Design

The scanner comprises the following main parts: film holder, mechanical feeder mechanism, intensity sensing device, position pulse generators and control panel.

(i) film holder:

This is designed to hold films measuring 20-150 mm (length); 112 mm (width); 0.2 mm (thick).

The scanned ^{area} film measures 100 x (5 to 135) mm. In the holder, the film is fixed so that it forms a circular cylinder, the axis of which is parallel to one of the edges of the film, see Fig. III.

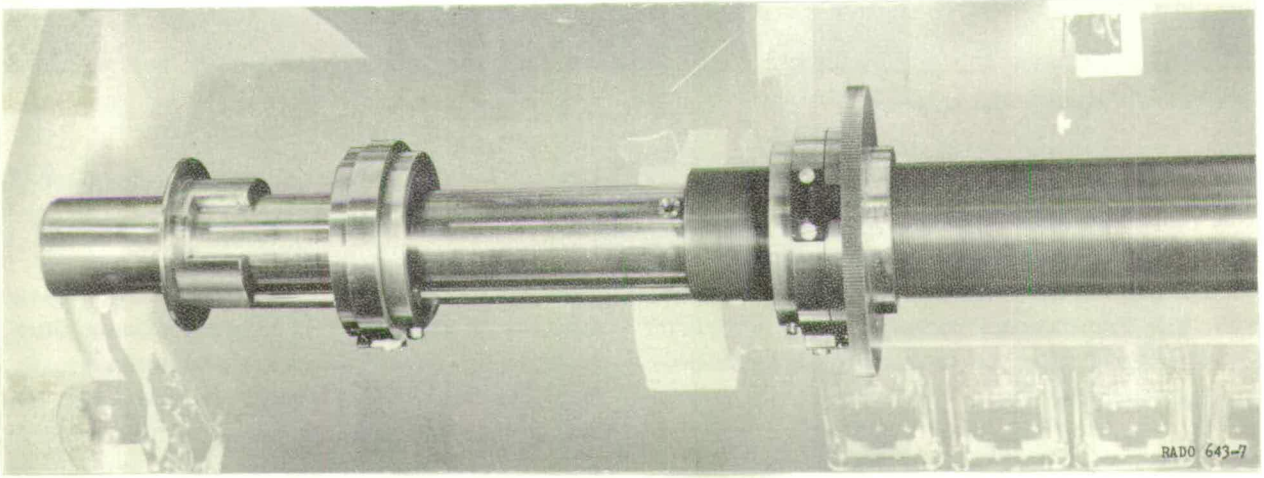
(ii) feeder mechanism:

The mechanical feeder mechanism is built on a heavy frame with a horizontally arranged tube which is fixed to the frame. Around the tube is mounted a high precision screw, and around the screw is the film holder. One end of this holder rests on a slide bearing, and at the other, it is internally threaded to fit the screw. Via an arrangement of gears driven by a synchronous electric motor the screw and holder are rotated at slightly different speeds. As a consequence the holder is translated along the screw meaning that a fixed sensing device scans the surface of the film in a spiral track. By means of electrically controlled clutches the translation per revolution may be chosen as either 45 μm or 90 μm .

It was decided that a track-width of 90 μm gave satisfactory results, and this has been used at all times. For the sake of defining film co-ordinates, the X direction was taken as lying along a track (i.e. around the circumference of the film holder), and the Y direction as parallel to the axis of the film holder. Thus 1 scanner unit in X is equivalent to 60 μm , and in Y is equivalent to 90 μm .

Fig. III

Film holder and feeder mechanism



To allow for quick "wind" and "re-wind" the screw can be locked. In this case, the translation of the holder depends only on the rotation speed and screw pitch. Limit switches protect the scanner against failures.

(iii) intensity sensor:

As shown in Fig. II, the measuring device consists mainly of a light source and a photomultiplier. The purpose of the instrument is to give information about the relative transmissions of successive small areas of the film.

The transmission is defined as the quotient

$$T = \frac{I}{I_0}$$

where I = intensity of the transmitted light beam, and

I_0 = intensity of the incident light beam.

The beam path is shown in Fig. IV.

The light source is a low voltage filament bulb supplied with stabilised direct current. The transmitted light beam (I) is reflected in a prism mounted in the fixed horizontal tube. At the end of the screw the beam falls on a photomultiplier giving a voltage which is directly proportional to the transmitted light beam. The incident light beam (I_0), which can be varied by an iris diaphragm, is kept constant during a scan.

(iv) computer connection:

The scanner is linked to an A/D converter, which in turn is linked to the computer. In the first stages of development this was a DEC PDP8 machine, but later a PDP15 machine was used.

Fig. IV

Diagram of the light beam path

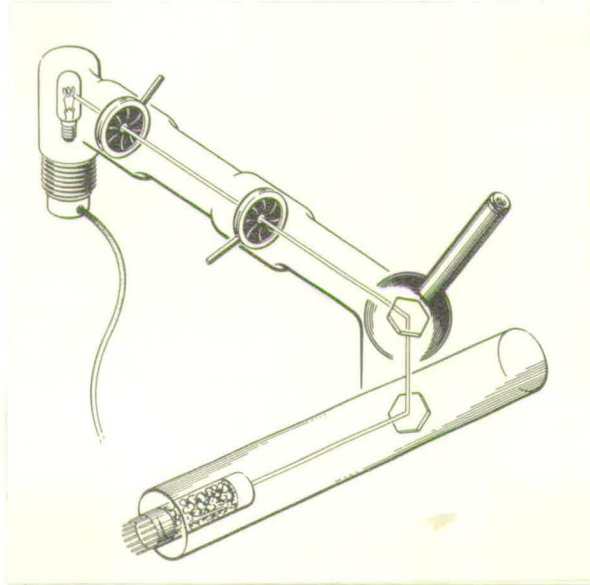
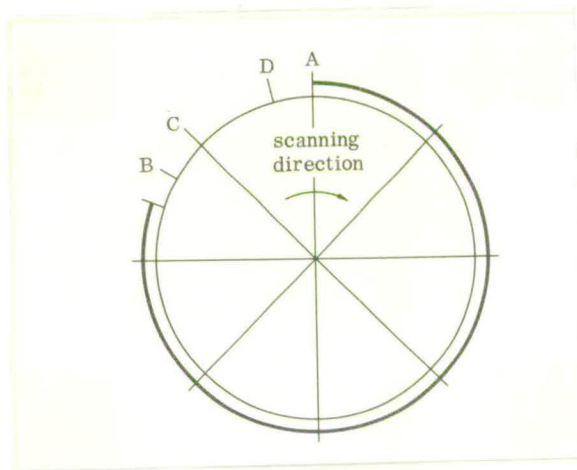


Fig. V

Diagram of the cross-section of the film holder



The information from the scanner is fed to the computer, as indicated in Fig. V. The film is positioned between A and B, and is scanned from A to B. As the scan passes A, a "beginning of track" pulse is transmitted to the computer indicating that information is being emitted. The pulse is counted and stored in a register holding the track number. This is followed by a "co-ordinate pulse", which starts the analogue-to-digital converter. The converted intensity value is fed to the computer which then adds one unit in the "co-ordinate" register. In this way, the successive intensity values along a track from A to B are read by the computer. The information following B is irrelevant, and is excluded by the computer. The scan then reaches C where a "stand by" pulse is transmitted in the form of a voltage step, which lasts until D when the computer waits for the beginning of the next track.

see fig 3
^

Operation

The actual process of data collection from a scan was carried out using a program written by Mrs. H.P. Drummond. The program reads the various voltages being generated by the scanner, and then writes these on IBM tape, together with the associated scanner co-ordinates, which can then be used for further processing on a larger computer. An additional feature of this program is that part of the data is also recorded on DEC tape which can be used at the end of a scan to generate a picture of the film on a video screen. This reconstruction of the film may be used both to check whether the data was correctly stored, and also to obtain approximate film co-ordinates for some of the spots.

III Software Development - PRECFIT

Throughout the work of this thesis, the computer software was continually being modified and updated as different computer facilities became available. As part of this development, a program PRECFIT was written which calculated the expected positions of spots on Buerger precession films. An input file was required which had on it the data from a film processed into spots with film co-ordinates also stored. Table I shows the rest of the input required to be given on c cards. Reciprocal cell were then calculated and printed. A further four numbers were then read from cards: XR1, XR2, YR1 and YR2. These defined the initial value of the lattice origin, XO, YO at the start of the least squares refinement.

$$XO = \frac{XR1 + XR2}{2} ; \quad YO = \frac{YR1 + YR2}{2}$$

They also defined the first and last tracks for the film in the X and Y directions.

Least Squares Refinement

The program then read up to 39 reflections with film co-ordinates and an associated serial number, and used these to refine the parameters XO, YO, F and T by least squares methods. At the end of each cycle, the new values were printed, together with the errors found. SIG (σ), the quantity minimised, was defined as:-

$$SIG = \frac{\Sigma (X_{OBS} - X_{CALC})^2 + (Y_{OBS} - Y_{CALC})^2}{NO-4}$$

where NO = no. of standard reflections used. Refinement continued until one of the following applied:-

TABLE I Card Input required for PRECFIT

<u>Variables Input</u>			<u>Meaning</u>		
A	B	C	a	b	c
AL	BE	GA	α	β	γ
	LAM		radiation wavelength		
	F		crystal-film distance (mms.)		
	T		angle of tilt of axis nearest to the horizontal		
	MU		μ - the precession angle		
	P		layer no.		
	Q		zone axis 1 = 100 2 = 010 3 = 001		
	IOUT		+1 if calculations from this program are to be written to an output file on disk, -1 if it is not		
	PATCH		no. of scanner points per spot used at the end of the program for modifying the intensities. It is assumed that all spots have N points, where N > PATCH		
	TCLIP		the fraction of data stored (e.g. 0.85)		

- (a) 10 cycles completed (NO CONVERGENCE printed)
- (b) SIG increases by more than 50% during a cycle (DIVERGENCE printed)
- (c) SIG decreases by less than 0.1% during a cycle (refinement stopped).

If (a) or (b) occurred, the job was terminated.

Calculations of spot positions

From precession geometry (48), the radii which define the limits of data collection on any film are given by:-

$$XIMAX = \sin(v) + \sin(\mu)$$

$$XIMIN = \sin(v) - \sin(\mu)$$

where μ = precession angle

and $v = \cos^{-1}(\cos(\mu) - \text{zeta})$

where $\text{zeta} = \text{layer number} \times \text{perpendicular reciprocal lattice distance between planes.}$

Fig. VI illustrates the above geometry.

If a variable DMIN is defined as $DMIN = \lambda/2\sin(\mu)$, then, if for example data collection is up the a-axis, $KM = \frac{b}{DMIN}$ and $LM = \frac{c}{DMIN}$ where KM and LM represent the maximum and minimum values of the k and l indices which may be observed on the film.

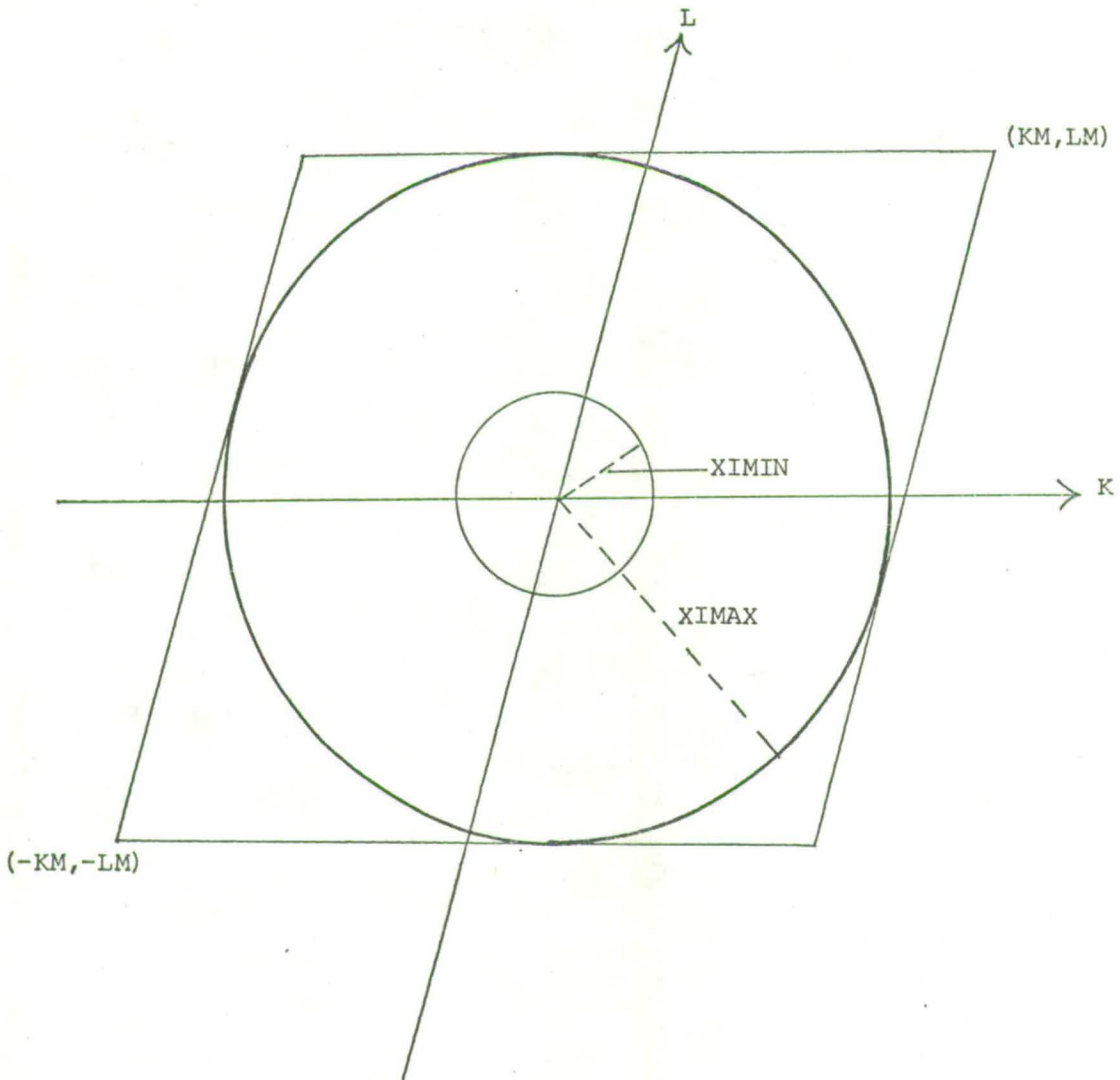
All the values of the cylindrical co-ordinates ξ and ϕ were calculated for points lying within the rhombus (KM,LM), (-KM,LM), (-KM,-LM), KM,-LM). If the point lay between XIMAX and XIMIN, its X and Y co-ordinates were calculated using the equations:

$$X = XO - (F \times \xi \times \sin \phi) \quad ; \quad Y = YO - (F \times \xi \times \cos \phi)$$

where ξ = distance of a point in reciprocal units from an axis in reciprocal space, i.e. one of the cylindrical co-ordinates.

Fig. VI

For any layer, reflections on a precession film
will lie within the area defined by the radii
XIMAX and XIMIN



$$= 4 \sin^2 \theta - \xi^2$$

where ξ = vertical distance in reciprocal units between horizontal lattice planes.

= layer number \times λ /axial cell dimension.

and ϕ = angular cylindrical co-ordinate required to define a point.

$$= \tan^{-1} \left(\frac{lc^* \sin \alpha^*}{kb^* + lc^* \cos \alpha^*} \right) - \text{when collecting up the a-axis}$$

these co-ordinates, together with the associated indices, were then stored in arrays.

Treatment of results

The positions where reflections might be found were sorted by indices using a routine SORT (written by Dr. R.O. Gould) and then printed out. This procedure was then repeated sorting the reflections by their Y co-ordinates.

These calculated positions were then used to specify the centre of frames. By comparing the areas bounded by these frames with the optical densities as stored on the scanner file, the intensities of all reflections on the film were calculated and stored on file.

IV Accuracy of spot intensities and positions

In order to see how accurate the film scanner was in measuring spot intensities and positions, test measurements were carried out using precession photographs of crystals of xylitol and lactoglobulin (Dr. D. Green, Dept. of Physics, University of Edinburgh).

(a) Intensities:

To compare intensities obtained from different scans, a reproducibility factor, R, was defined as

$$R = \frac{\sum |I_1 - I_2|}{\sum I_2} \times 100$$

In arriving at a value of R, no spot was used if any scanner reading gave an optical density greater than 2.50.

A film of xylitol was scanned twice without removing the film from its holder in between scans. All instrument settings were kept the same. 27 reflections were compared, and the conclusions reached are shown in Table II. The intensities agreed with each other giving R = 3.8%, and there was no overall scale-factor between the 2 data sets. The table also groups the reflections by their respective intensities.

A second film of xylitol was also scanned twice, the film being remounted on the scanner between scans. Again, all instrument settings were kept the same. Table III shows the conclusions reached by comparing 33 reflections. Agreement between intensities was not quite as good, R = 5.0%, but once again, there was no overall scale-factor between the sets of data.

As a comparison with another method, a film of lactoglobulin was scanned both on the SAAB scanner and a Joyce-Loebl micro-densitometer.

TABLE II

For 27 independent observations:

$$\Sigma | I_1 - I_2 | = 833$$

$$\Sigma I_2 = 21863$$

$$\therefore R = 3.8\%$$

Grouping the observations by intensities:

$I_{\text{obs.}}$ range	100-800	800-1600	> 1600
number in range	14	8	3
average $\Delta I/I$ (1)	.026	.015	.010
standard deviation	.035	.016	.016

(1) $\Delta I/I$ = error of an individual observation divided by the average intensity for the group.

TABLE III

For 33 independent observations:

$$\Sigma | I_1 - I_2 | = 2018$$

$$\Sigma I_2 = 39988$$

$$\therefore R = 5.0\%$$

Grouping the observations by intensities:

$I_{\text{obs.}}$ range	100-1000	1000-2000	2000-4000
number in range	19	9	5
average $\Delta I/I$.04	.03	.02
standard deviation	.05	.035	.026

105 intensities were compared and the results listed in Table IV. The agreement here gave $R = 9.5\%$. Allowing for the fact that a micro-densitometer was used, rather than the more accurate diffractometer, the results obtained confirmed the fact that the scanner was quite capable of giving reproducible intensities to a tolerable accuracy, although not to the accuracy of a diffractometer.

The tests showed that absolute errors increase as the intensity increases, but not linearly, whereas percentage errors decrease. Also, as would be expected, no overall scale-factor was observed between 2 sets of data obtained from the scanner off the same film.

(b) Positions:

Four different tests were carried out to determine how accurate the scanner was in determining the co-ordinates of reflections.

A photograph of xylitol was scanned twice without being removed from the scanner in between scans. As an automatic rewind was used to ensure that the scan started from as near as possible the same starting point, the absolute film co-ordinates for successive runs were able to be compared. Table V shows the mean differences in X and Y co-ordinates for 22 different reflections; these were 0.11 and 0.52 scanner units respectively.

Next, two similar films of xylitol, differing only in exposure length, were then scanned. Since it was not possible to guarantee that the two films would be inserted into the film holder with the same orientation, the only meaningful comparison was to test the reproducibility of distances between reflections. Table VI shows that for 12 different measurements, the mean difference in distance between any two reflections was 33 μm .

TABLE IV

For 105 independent observations:

$$\Sigma | I_{\text{obs.}} - I_{\text{pub.}} | = 3861$$

$$\Sigma I_{\text{pub.}} = 40635$$

$$\therefore R = 9.5\%$$

where $I_{\text{obs.}}$ = reflection measured by SAAB scanner

and $I_{\text{pub.}}$ = reflection measured by micro-densitometer

Grouping the observations by intensities:

$I_{\text{obs.}}$ range	100-500	500-1000	>1000
number in range	82	16	7
average $\Delta I/I$.13	.09	.07
standard deviation	.08	.04	.05

TABLE V

For 22 independent observations:

mean difference in X co-ordinate = 0.11(.09) scanner units

mean difference in Y co-ordinate = 0.52(.14) scanner units.

1 scanner unit in X direction = 60 μm , and

1 scanner unit in Y direction = 90 μm .

TABLE VI

For 12 independent observations:

mean difference in distance between any 2 reflections = 33(28) μm .

TABLE V

For 12 independent observations:

mean difference in distance between any 2 reflections = 43(32) μm .

Note: errors quoted in the above Tables are standard deviations.

In a third test, a film of xylitol was scanned twice, but was removed and remounted in between scans. Once again, reproducibility was measured by the constancy of distances between reflections. Table VII indicates that the mean difference between measurements was 43 μm .

Finally, to examine the constancy of reciprocal lattice translations, 14 distances were measured corresponding to unit translations in the X direction and 17 corresponding to translations of 2 units in the Y direction. Table VIII shows the results obtained. In order to compare with published cell dimensions (49), Y/X was related to a^*/b^* (thus eliminating absolute errors such as film shrinkage, etc.).

Mean distance between adjacent spots in the X direction

$$= 10224 \mu\text{m} (\sigma = 36)$$

Mean distance between adjacent spots in Y direction

$$= 11092 \mu\text{m} (\sigma = 14)$$

$$\therefore Y/X = 1.085 (\sigma = 0.004)$$

From the published data, $a^*/b^* = 1.082$. These results show good agreement with the calculated value of a^*/b^* , and also that the standard deviations from a regular lattice are less than one scanner unit.

TABLE VIII

For 39 independent observations:

mean distance between adjacent spots in X direction = 10224(36) μm .

mean distance between adjacent spots in Y direction = 11092(14) μm .

$$\therefore Y/X = 1.085(.004)$$

Errors are standard deviations.

The published value for $a^*/b^* = 1.082$.

APPENDIX II

Observed and Calculated Structure

Factors for L-Leucine

Each column lists: H, $10F_o$, $10F_c$.

An asterisk signifies a reflection too weak to measure.

	H,0,0		12	140	152	4	66	48
						5	28	12
3	75	119		H,0,3		6	38	49
4	691	689				7	50	49
5	611	712	-3	51	63	8	56	56
6	559	463	-2	59	75	9	28*	10
7	110	108	-1	62	68	10	29*	5
8	87	80	0	30	31	11	72	72
9	195	182	1	111	84	12	51	44
10	133	113	2	31	13	13	29*	11
11	99	93	3	121	115	14	27	13
12	85	78	4	49	38	15	25*	25
13	77	68	5	48	34	16	22*	12
			6	74	62	17	18*	21
	H,0,1		7	130	143			
			8	64	61		H,0,6	
3	74	77	9	43	49			
4	125	93	10	26*	17	-4	87	104
5	101	91				-3	70	69
6	107	103		H,0,4		-2	24	15
7	76	65				-1	345	297
8	65	59	-3	153	157	0	228	193
9	79	68	-2	270	250	1	125	119
11	27*	17	-1	124	133	2	101	102
12	28*	34	0	344	314	3	108	128
13	83	89	1	298	262	4	105	75
14	29*	32	2	432	398	5	25*	20
15	28*	3	3	339	325	6	97	94
16	26*	26	4	173	163	7	77	81
17	23*	4	5	21*	41	8	28*	65
18	19*	4	6	334	289	9	29*	3
10	25*	35	7	337	297	10	83	94
			8	257	214	11	59	58
	H,0,2		9	89	101			
			10	27*	16		H,0,7	
-3	349	350	11	29*	42			
-2	335	352	12	85	127	-3	55	58
-1	92	126	13	113	119	-2	27*	14
0	63	72	14	53	63	-1	38	30
1	768	883				0	26*	14
2	68	100		H,0,5		1	83	64
3	548	456				2	37	28
4	695	535	-4	65	73	3	27*	24
5	63	9	-3	54	62	4	27*	12
6	147	109	-2	63	57	5	28*	4
7	54	54	-1	49	29			
8	338	324	0	39	8		H,0,8	
9	127	125	1	36	14			
10	99	107	2	94	93	-3	82	97
11	27*	36	3	45	28			

H ₂ O, 8		13	83	76	H ₂ O, -8			
0	195	214			1	29*	29	
1	211	205			2	29*	12	
2	29*	35	4	68	64	4	203	210
3	29*	29	5	117	123	5	166	157
4	29*	2	6	71	76	6	46	50
5	29*	11	7	23	25	7	29*	17
6	29*	19	8	49	38	8	80	82
7	29*	7	9	63	52	9	85	113
8	29*	31	10	27*	10			
9	29*	44	11	29*	4			
10	28*	49	12	29*	2			
11	62	54	13	29*	39	1	29*	15
			14	28*	24	2	58	61

H ₂ C, 10		H ₂ O, -4		H ₂ O, -10				
3	55	58	4	21*	16			
4	77	72	5	27	13	0	79	0
5	27*	18	6	103	118	1	59	50
6	26*	18	7	24*	33	2	27*	56
7	25*	28	8	37	34	3	27*	6
8	51	37	9	39	28	4	26*	16
9	47	34				5	53	37
						6	51	50

H ₂ O, -1		H ₂ O, -5		H ₂ O, -12				
2	54	56	5	72	69			
4	41	41	6	25*	1			
5	16*	5	7	26*	14	-2	42	79
6	18*	16	8	44	52	-1	50	66
7	20*	12				0	54	5
8	22*	1				1	46	72
9	24*	19				3	50	68
10	26*	8	5	118	126	4	47	35
11	51	55	6	87	89			
12	86	102	7	66	53			
13	29*	34	8	129	123			

H ₂ C, -2		H ₂ O, -6		H ₂ O, -7		H, 1, 0		
4	201	163	9	93	101	3	162	168
5	209	187	10	72	81	4	109	79
6	31	63	11	61	61	5	176	161
7	103	121	12	79	102	6	122	131
8	54	47	13	25*	14	7	45	54
9	25	35				8	60	56
10	79	77				9	50	73
11	48	49	4	48	63	10	61	57
12	41	56	5	60	64	11	81	84
						12	42	48

	H,1,-6			H,1,8			8	114	91
							9	31*	34
4	21*	32	-1	76	74		10	33*	26
3	32	47	1	68	64		11	35*	35
			2	79	77				
	H,1,6		3	54	55		H,2,1		
			4	54	44				
-2	20*	16	5	33	38	-12	53	58	
-1	41	38	6	37	40	-11	92	107	
0	36	25	7	23*	33	-10	74	66	
1	40	27	8	23*	30	-9	32*	19	
			9	23*	17	-8	101	90	
	H,1,-7			H,1,-9			-7	83	84
9	68	73				-6	54	57	
8	80	84	3	76	40	-5	197	178	
7	77	82	2	73	89	-4	99	109	
6	36	42	-1	102	112	-3	80	62	
5	75	79	-2	80	98	-2	59	56	
4	98	103				3	111	130	
3	103	112		H,1,9		4	148	149	
2	126	123				5	208	199	
1	55	63	-1	73	89	6	120	113	
0	105	100		H,1,-9		7	60	61	
						8	37	38	
	H,1,7					9	81	52	
			0	88	55	10	42	42	
1	124	103				11	79	66	
2	124	127		H,1,9			H,2,2		
3	87	105							
4	86	108	3	80	91	-12	53	37	
5	22*	32	4	61	66	-11	36*	23	
6	114	114	5	60	45	-10	78	89	
7	116	115	6	60	56	-9	150	143	
8	49	64	7	47	58	-8	234	215	
9	54	57	8	45	52	-7	172	147	
10	43	48	9	20*	25	-6	26*	14	
11	47	48				-5	120	95	
12	34	41		H,1,-10		-4	224	239	
13	52	43				-3	266	265	
			2	54	26	-2	186	191	
	H,1,-8		1	40	26	-1	55	61	
5	61	32		H,2,0		0	56	85	
4	77	70				1	57	72	
3	52	78	3	142	143	2	135	159	
2	56	47	4	86	88	3	155	190	
0	48	31	5	32	28	4	243	248	
			6	146	129	5	204	216	
			7	39	43	6	154	177	
						7	27*	35	

	H,2,2		2	113	113	3	92	87
			3	66	69	4	150	162
8	136	112	4	50	25	5	120	118
9	193	160	5	53	48	6	98	77
10	133	124	6	101	104	7	70	69
11	35*	27	7	142	131	8	45	42
12	36*	25	8	56	30	9	103	88
			9	59	47	10	79	78
	H,2,3		10	35*	37			

-11	79	68
-10	35*	35
-9	34*	23
-8	32*	36
-7	97	82
-6	141	137
-5	66	54
-4	79	66
-3	23*	14
-2	57	67
-1	150	158
0	58	67
1	41	52
2	60	68
3	42	31
4	59	52
5	133	126
6	67	56
7	83	69
8	39	36
9	41	26
10	60	58
11	62	47
12	62	49

	H,2,5	
-11	67	48
-10	53	69
-9	36*	60
-8	52	22
-7	60	63
-6	57	42
-5	91	87
-4	61	66
-3	102	78
-2	43	41
-1	91	104
0	53	35
1	110	95
2	140	137
3	114	104
4	37	32
5	46	49
6	83	81
7	73	80
8	51	49
9	35*	13
10	45	29

	H,2,7	
-5	36*	35
-4	36*	37
-3	35*	24
-2	35*	37
-1	35*	28
0	34*	38
1	34*	7
2	34*	16
3	35*	38
4	35*	43
5	35*	13
6	36*	38
7	36*	34
8	36*	26
9	36*	13

	H,2,4	
-11	45	23
-10	36*	5
-9	52	53
-8	84	79
-7	74	88
-6	106	119
-5	66	60
-4	146	130
-3	131	119
-2	37	35
-1	25*	35
0	185	194
1	147	174

	H,2,6	
-10	76	25
-9	93	75
-8	72	94
-7	89	75
-6	45	62
-5	90	39
-4	96	81
-3	130	89
-2	148	123
-1	79	120
0	82	76
1	78	77
2	32*	9

	H,2,8	
-3	68	51
-2	62	55
-1	43	28
0	45	45
1	45	39
2	36*	23
3	36*	17
4	36*	22
5	36*	28

	H,2,9	
-3	34*	22
-2	35*	18
-1	35*	53
0	35*	32
1	35*	38
2	35*	48

	H,2,10		9	19*	33	4	63	55
			10	20*	29	5	16*	16
-3	30*	43				6	48	40
-2	46	45		H,3,2		7	42	40
-1	69	32				8	93	92
0	38	43	-11	61	62	9	59	66
1	47	67	-10	51	56	10	20*	21
2	70	51	-9	36	23			
3	78	24	-8	92	73		H,3,4	
4	59	44	-7	87	78			
5	30*	64	-6	81	74	-9	61	51
			-5	180	164	-8	40	36
	H,3,0		-4	113	103	-7	96	94
			-3	48	42	-6	44	24
1	85	75	-2	80	72	-5	67	64
2	144	158	-1	112	103	-4	92	85
3	164	189	0	85	106	-2	119	110
4	51	51	1	86	88	-1	39	35
5	102	100	2	91	91	-3	37	29
6	92	92	3	109	122	0	39	43
7	67	58	4	82	71	1	46	45
8	18*	32	5	101	119	2	77	73
9	19*	5	6	90	84	3	79	72
10	20*	7	7	91	81	4	82	76
			8	104	105	5	49	57
	H,3,1		9	19*	22	6	18*	22
			10	20*	8	7	57	54
-15	29	36				8	20*	34
-14	56	46		H,3,3		9	60	52
-13	54	37				10	20*	28
-12	47	45	-16	26	11			
-11	38	28	-15	14*	28		H,3,5	
-10	90	73	-14	48*	44			
-9	95	93	-13	18*	32	-12	48	32
-8	68	59	-12	19*	14	-11	58	57
-7	17*	21	-11	20*	12	-10	19*	30
-6	0	3	-10	45	41	-9	20*	23
-5	92	77	-9	99	104	-8	47	57
-4	153	139	-8	118	91	-7	60	41
-3	115	95	-7	41	29	-6	56	59
-2	72	63	-6	66	57	-5	82	70
-1	160	159	-5	47	36	-4	35	29
1	93	89	-4	116	107	-3	63	59
2	103	94	-3	118	111	-2	50	51
3	129	130	-2	39	41	-1	93	86
4	137	146	-1	54	41	0	113	116
5	116	119	0	37	55	1	99	93
6	34	27	1	59	56	2	74	95
7	70	68	2	66	67	3	72	84
8	72	71	3	66	74			

	H,3,5		2	20*	23	13	37	27
			3	57	63	14	20	22
4	137	141	4	61	59			
5	122	127	5	64	71		H,4,1	
6	95	99	6	60	54			
7	44	47	7	51	47	-11	55	50
8	60	67	8	20*	35	-10	65	71
9	86	97	9	65	65	-9	49	51
10	51	59	10	51	57	-8	33	37

	H,3,6			H,3,8				
-11	37	31	-9	32	19	-4	51	46
-10	18*	39	-5	44	40	-3	60	56
-9	61	46	-4	19*	29	-2	48	47
-8	20*	31	-3	50	45	-1	41	41
-7	85	92	-2	56	40	0	34	41
-6	82	69	-1	20*	33	1	53	84
-5	38	47	0	37	26	2	27	31
-4	113	110	1	20*	31	3	47	45
-3	83	79	2	20*	16	4	68	72
-2	45*	46	3	20*	23	5	67	64
-1	36	17				6	52	36
0	19*	20		H,3,9		7	25*	21
1	71	67				8	48	51
2	81	92	-8	12*	14	9	34	35
3	82	85	-7	14*	17	10	66	64
4	83	80	-6	34	23	11	33	37
5	56	47	-5	33	27			
6	60	63	-4	32	40		H,4,2	
7	61	58	-3	22	39			
8	70	64	-2	18*	15	-13	27	34
9	40	43	-1	18*	18	-12	30	32
10	19*	8	0	47	42	-11	32	31
11	34	32	1	56	44	-10	27*	3
12	17*	20				-9	43	52

	H,3,7			H,4,0				
-9	17*	24	1	24	20	-6	31	20
-8	41	46	2	28	29	-5	64	61
-7	54	50	3	36	34	-4	68	62
-6	20*	13	4	19	11	-3	49	42
-5	20*	26	5	39	25	-2	29	32
-4	57	46	6	48	41	-1	31	42
-3	40	45	7	55	53	0	42	46
-2	64	57	8	63	51	1	41	40
-1	70	66	9	43	52	2	18*	11
0	38	35	10	27*	24	3	35	35
1	40	38	11	33	35	4	51	48
			12	40	42			

	H,4,2		3	30	21	9	31	32
			4	68	72			
5	36	24	5	65	72		H,4,7	
6	24*	23	6	42	28			
7	25	21	7	27*	13	-6	24	22
8	26*	18	8	27*	14	-5	40	43
9	49	44				-4	62	65
10	34	37		H,4,5		-3	33	42
						-2	26	24
	H,4,3		-9	25	29	-1	26	31
			-8	26*	8	0	65	60
-12	36	43	-7	33	30	1	59	60
-11	31	28	-6	78	68	2	33	30
-10	33	37	-5	34	40	3	42	44
-9	34	31	-4	56	50	4	33	33
-8	49	46	-3	67	55	5	33	40
-7	113	134	-2	120	130	6	46	52
-6	99	98	-1	99	101	7	31	34
-5	84	77	0	25*	22			
-4	60	65	1	70	77		H,4,8	
-3	214	207	2	91	98			
-2	177	170	3	92	99	-5	22	31
-1	79	76	4	59	64	-4	29	25
0	20	19	5	56	59	-3	43	39
1	82	75	6	56	59	-2	30	43
2	163	175	7	43	47	-1	31	33
3	93	105	8	34	44	0	31	29
4	29	32	9	33	29	1	40	40
5	39	52	10	25*	22	2	45	53
6	53	41				3	60	63
7	48	25		H,4,6		4	53	45
8	34	32				5	43	34
9	27	26	-9	28	28	6	50	42
10	26*	13	-8	24*	6	7	39	39
			-7	25*	29	8	25	37
			-6	26*	38			
			-5	43	44		H,4,9	
			-4	49	36			
-10	25	26	-3	27	17	-4	43	49
-9	33	22	-2	27	25	-3	42	45
-8	27*	17	-1	34	44	-2	20*	6
-7	27*	7	0	60	62	-1	38	39
-6	56	52	1	49	46	0	47	44
-5	92	87	2	27	39	1	51	47
-4	98	93	3	43	39	2	34	30
-3	68	60	4	27	29	3	33	34
-2	39	34	5	27	36	4	48	53
-1	91	101	6	27	31	5	35	40
0	108	115	7	26*	20			
1	82	80	8	41	44			
2	43	45						

APPENDIX III

Observed and Calculated Structure

Factors for DL-Leucine

Each column lists: K , lOF_o , lOF_c .

An asterisk signifies a reflection too weak to measure.

	0, K, 0		13	13*	-18	-8	22	-26
			14	22	25	-7	24	17
2	38	-29	15	12*	-13	-6	76	-77
3	28	16	16	10*	12	-5	22	26
4	315	-340	17	9*	-18	-4	27	29
5	378	392				-3	71	-63
6	283	-250		2, K, 0		-2	74	63
7	21	17				-1	141	-136
8	10*	3	-16	9*	6	0	82	75
9	133	-126	-15	11*	3	1	194	196
10	120	108	-14	55	-51	2	111	-117
11	56	59	-13	78	83	3	42	35
12	29	16	-12	94	-92	4	71	-65
13	32	-27	-11	13*	1	5	20	-25
14	39	-29	-10	23	31	6	91	87
15	12*	14	-9	55	-43	7	76	-79
16	21	30	-8	110	128	8	13*	16
17	23	-34	-7	133	-135	9	13*	14
			-6	179	180	10	74	-74
	1, K, 0		-5	55	-35	11	65	68
			-4	93	-82	12	24	30
-16	11*	-2	-3	133	109	13	25	-27
-15	12*	-16	-2	241	-209	14	23	21
-14	42	41	-1	125	144	15	47	-51
-13	95	-90	0	261	-253			
-12	138	133	1	74	66		4, K, 0	
-11	23	-33	2	154	158			
-10	103	-99	3	110	-105	-14	37	35
-9	95	92	4	80	84	-13	39	-39
-8	205	-199	5	15	-13	-12	11*	-5
-7	70	75	6	66	59	-11	67	63
-6	99	69	7	11*	-4	-10	87	-56
-5	16	-16	8	23	-26	-9	17	23
-4	235	239	9	24	-28	-8	19	-31
-3	243	-266	10	29	28	-7	26	-29
-2	41	47	11	70	-66	-6	13*	21
-1	362	380	12	13*	2	-5	19	25
0	164	-191	13	68	65	-4	13*	16
1	41	-23	14	57	-52	-3	28	20
2	242	-246	15	46	43	-2	68	-62
3	104	-81				-1	13*	-8
4	131	133		3, K, 0		0	142	135
5	161	-126				1	114	-108
6	149	167	-15	34	34	2	42	41
7	30	-30	-14	11*	-10	3	73	-63
8	27	-24	-13	12*	1	4	25	-36
9	56	54	-12	18	-21	5	115	109
10	12*	2	-11	13*	1	6	109	-101
11	68	62	-10	77	83	7	107	99
12	97	-89	-9	13*	-20			

	4,K,0		1	247	-232	-1	105	112
			2	52	83	0	297	-343
8	50	-42	3	208	-197	1	108	94
9	45	-35	4	161	-130	2	77	42
10	59	59	5	26	-24	3	80	-94
11	25	-31	6	145	126	4	92	100
12	41	47	7	11*	-8	5	10*	-12
13	66	-52	8	25	21	6	75	75
			9	60	-56	7	58	40
	5,K,0		10	32	34	8	86	-72
			11	126	125	9	55	45
-11	31	-42	12	119	-101	10	14*	3
-10	9*	12	14	42	-37	11	87	-74
-9	10*	12				12	15*	12
-8	20	-32		0,K,1		13	15*	-6
-7	41	44				14	15*	19
-6	22	-29	0	314	300	15	14*	-2
-5	38	36	1	223	202			
-4	13*	2	2	280	-297		1,K,1	
-3	53	-52	3	223	239			
-2	24	33	4	174	-172	-15	21	-29
-1	13*	-11	5	259	279	-14	17*	17
0	13*	7	6	10*	-19	-13	49	-41
1	13*	-14	7	210	-229	-12	68	69
2	17	-17	8	110	107	-11	112	106
3	40	37	9	145	-129	-10	113	-113
4	13*	-20	10	84	73	-9	13*	-3
5	13*	9	12	15*	-4	-8	98	-88
6	17	20	13	32	39	-7	43	44
7	13*	-26	14	52	-55	-6	91	75
8	19	21	15	39	39	-5	186	-172
9	14	-29	16	11*	17	-4	82	69
						-3	133	-120
	6,K,0			1,K,-1		-2	56	41
-6	25	27	-16	17	-40	-1	283	336
-5	29	-31	-15	18	12	1	87	-60
-4	9*	10	-14	14*	5	2	221	-265
-3	9*	11	-13	22	-30	3	56	-33
-2	21	-29	-12	42	40	4	177	162
-1	63	56	-11	64	-70	5	69	-78
0	84	-81	-10	15*	-10	6	28	-42
1	62	62	-9	69	63	7	69	-61
2	10*	8	-8	103	-89	8	13*	2
3	52	-47	-7	49	44	9	85	87
4	59	66	-6	125	121	10	24	-30
5	71	-77	-5	54	-58	11	72	87
			-4	114	113	12	35	-36
	0,K,-1		-3	94	-101	13	68	-57
			-2	29	-12	14	39	52

	1, K, 1		-2	134	-124	-6	78	-79
			-1	149	153	-5	87	101
15	13*	-30	2	297	298	-4	51	-56
16	16	34	3	215	-195	-3	118	-113
			4	145	141	-2	115	122
	2, K, -1		5	48	29	6	94	109
			6	159	-134	7	96	-102
-15	23	-21	7	222	216	8	15*	10
-14	13*	4	8	132	-128	9	15*	-7
-13	23	37	9	39	46	10	36	-21
-12	66	-74	10	59	43			
-11	34	39	11	79	-75		4, K, -1	
-10	15*	17	12	15*	7			
-8	14*	27	13	15*	-15	-12	9*	-8
-8	39	27				-11	11*	13
-7	20	19		3, K, -1		-10	13*	-18
-6	50	-56				-9	14*	-3
-5	40	-43	-12	13*	17	-8	32	41
-4	12*	8	-11	14*	2	-7	95	-86
-3	11*	-4	-10	15*	-2	-6	75	65
-2	103	87	-9	40	32	-5	25	27
-1	252	-245	-8	32	-45	-4	44	-45
0	77	94	-7	15*	15	-3	113	99
1	91	86	-6	96	-91	-2	163	-155
2	49	37	-5	15*	16	-1	119	101
3	116	113	-4	119	112	0	15*	-6
4	173	-173	-3	50	-50	1	105	-97
5	115	116	-2	42	37	2	140	138
6	115	-116	-1	86	-78	3	138	-131
7	38	32	0	34	41	4	70	63
8	64	55	1	133	112	5	15*	-1
9	99	-90	2	101	-103	6	15*	-24
10	44	43	3	28	42	7	94	87
11	86	-93	4	43	-50	8	88	-78
12	113	99	5	99	-90	9	14*	13
13	15*	21	6	112	106	10	13*	13
			7	29	-32	11	11*	-7
	2, K, 1		8	34	40			
			9	15*	-3		4, K, 1	
-13	15*	11	10	87	-90			
-12	68	58	11	94	114	-11	94	102
-11	93	-84				-10	31	-32
-10	14*	-11		3, K, 1		-9	15*	-6
-9	60	-52				-8	15*	-10
-8	51	51	-12	15*	10			
-7	12*	18	-11	73	-73		5, K, -1	
-6	11*	-11	-10	98	103			
-5	162	147	-9	15*	-7	-8	10*	-8
-4	165	-158	-8	38	-27	-7	24	38
-3	170	166	-7	82	69			

2,K,2

-12	78	73
-11	16*	17
-10	164	-146
-9	113	76
-8	118	-86
-7	134	122
-6	19	-32
-5	185	-175
-4	197	176
-3	99	-76
-2	166	167
-1	8*	19
2	78	-87
3	94	104
4	31	-35
5	47	44
6	141	-158
7	62	79
8	81	67
9	47	-43
10	56	67
11	60	-57
12	15*	17
13	14*	-8

3,K,-2

-12	16	25
-11	37	-37
-10	14*	2
-9	30	18
-8	15*	-5
-7	16*	-11
-6	42	-35
-5	45	42
-4	39	28
-3	16*	1
-2	16*	5
-1	15*	-20
0	15*	-8
1	15*	-6
2	15*	-6
3	29	38
4	60	-52
5	32	-28
7	18*	-6
11	23	35

3,K,2

-13	15*	13
-12	16*	-5
-11	24	-36
-10	24	-29
-9	38	40
-8	14*	15
-7	14*	19
-6	33	-26
-5	25	33
-4	34	33
-3	40	-51
-2	32	25
-1	11*	0

4,K,-2

-10	17	-25
-9	21	25
-8	12*	3
-7	30	-40
-6	78	80
-5	58	-60
-4	24	18
-3	15*	1
-2	25	-36
-1	65	60
0	80	-73
1	33	28
2	16*	16
3	15*	-13
4	15*	13
5	15*	4
6	14*	3
7	14*	-15
8	13*	7
9	24	-16

4,K,2

-12	14*	-9
-11	15*	-24
-10	72	87
-9	56	-64
-8	28	35
-7	28	-27
-6	15*	2
-5	52	65
-4	105	-116

-3	47	40
-2	30	-27
-1	26	31

5,K,-2

-4	10*	3
-3	11*	-14
-2	38	45
-1	24	-29
0	12*	-5
1	13	22
2	25	-26
3	15	27
4	11*	0
5	9*	-11

0,K,-3

1	31	-40
2	29	34
3	24	-36
4	59	59
5	92	97
6	116	-110
7	42	52
8	57	-59
9	47	58
11	69	-81
12	47	51

0,K,3

0	7*	-2
1	82	-66
2	84	64
3	73	-52
4	20	16
5	44	-35
6	10*	10
7	137	114
8	103	-95
9	39	44
10	12*	-12
11	11*	-10
12	15	26

	1, K, -3	
-12	10*	26
-11	11*	-6
-10	11*	7
-9	19	-27
-8	24	24
-7	81	61
-6	93	-67
-5	11*	-22
-4	34	-28
-3	10*	12
-2	54	37
-1	25	-10
0	36	22
1	32	-30
2	9*	-4
3	57	56
4	44	52
5	48	-46
6	67	-74
7	11*	-8
8	40	42
9	12*	11
10	12*	-10
11	12*	-8
12	11*	-11
13	21	26
14	14	-6

10	12*	13
11	12*	-4
	2, K, -3	
-10	10*	-15
-9	11*	-14
-8	51	54
-7	47	-51
-6	12*	-1
-5	12*	-5
-4	12*	7
-3	38	33
-2	11*	-5
-1	59	51
0	67	-73
1	11*	19
2	32	-30
3	45	44
4	11*	18
5	120	-117
6	80	83
7	42	-42
8	56	44
9	12*	23
10	44	-53
11	52	51
12	36	-48

7	98	-100
8	103	94
9	12*	14
10	34	-44
	3, K, -3	
-9	8*	6
-8	9*	11
-7	23	-33
-6	41	45
-5	11*	-7
-4	11*	-16
-3	17	23
-1	14	16
0	14	-18
1	17	-27
2	36	41
3	17	-14
4	12*	-15
5	40	42
6	29	-22
7	11*	11
8	10*	-4
9	10*	-16

	1, K, 3	
-11	12*	-10
-10	36	43
-9	37	-38
-8	52	51
-7	9*	1
-6	8*	-2
-5	81	89
-4	179	-167
-3	20	29
-2	44	61
2	10	22
3	89	86
4	87	-69
5	69	69
6	10*	25
7	88	-93
8	33	34
9	12*	-17

	2, K, 3	
-12	12*	4
-11	12*	27
-10	38	-46
-9	11*	17
-8	10*	17
-7	10*	-18
-6	64	86
-5	246	-232
-4	54	81
-3	59	47
-2	21	-13
-1	127	122
0	161	-180
1	159	157
2	76	-74
3	8*	17
4	85	68
5	114	-102
6	21	34

	3, K, 3	
-11	12*	13
-10	39	-47
-9	12*	-8
-8	75	76
-7	53	-55
-6	10*	5
-5	61	-44
-4	50	46
-3	119	107
-2	110	-97
-1	39	43
	4, K, -3	
-6	7*	-9
-5	8*	-17
-4	8*	9
-3	25	-31
-2	32	41
-1	19	-23
0	10*	16

4,K,-3

1	10*	-2
2	10*	-13
3	9*	11
4	9*	-1
5	19	34
6	31	-44

4,K,3

-12	31	38
-11	71	-75
-10	57	53
-9	12*	17
-8	31	-50
-7	79	103
-6	156	-145
-5	134	133
-4	11*	-11
-3	126	-119
-2	139	146
-1	143	-149

5,K,3

-9	11*	27
-8	11*	-13
-7	11*	-27
-6	43	60
-5	48	-36
-4	22	-33
-3	24	29
-2	24	-14
-1	22	34

0,K,-4

1	37*	22
2	34*	13
3	98	-108
4	191	200
5	106	-94
6	35*	-6
7	35*	12
8	74	-83
9	91	95
10	47	-51

0,K,4

0	75	-64
1	123	127
2	83	-90
3	35*	7
4	35*	10
5	49	-55

0,K,-5

1	74	59
2	73	-61
3	33*	8
4	53	45
5	64	-52
6	60	37
7	30*	-21

0,K,5

0	66	-61
1	74	80
2	32*	-7
3	64	-63
4	57	60
5	29*	-49

1,K,-4

-6	28	-36
-5	48	52
-4	59	-64
-3	25*	24
-2	25*	25
-1	25*	1
0	45	47
1	66	-72
2	25*	-8
3	64	56
4	50	-31
5	25*	13
6	41	-34
7	25*	-10
8	43	32
9	24*	-23
10	43	51

1,K,4

-6	25*	3
-5	85	91
-4	39	-47
-3	24*	14
-2	24*	-23
-1	24*	-19
0	56	47
1	76	-75
2	25*	31
3	25*	9
4	35	-23
5	34	21

1,K,-5

-5	44	31
-3	20*	12
-2	21*	26
-1	21*	-25
0	30	26
1	33	-33
2	22*	2
3	25*	24
4	42	-45
5	31	37
6	20*	-4
7	19*	-11
8	18*	8

1,K,5

-3	25*	10
-2	25*	-33
-1	25*	2
0	46	48
1	25*	-28
2	25*	-11
3	24*	-10

2,K,-4

-5	40*	-24
-4	51	40
-3	53	-53
-2	60	58
-1	44*	-20
0	44*	-34
1	56	36
2	51	-53
3	62	58

2,K,-4

4	60	-43
5	43*	11
6	42*	36
7	40*	-42
8	39*	25

2,K,4

-8	46*	-7
-7	45*	35
-6	45*	-44
-5	48	46
-4	98	-94
-3	43*	44
-2	43*	22
-1	42*	-32
0	43*	0
1	43*	-19
2	90	64
3	44*	-15
4	45*	11
5	46*	-23
6	46*	28
7	46*	-40
8	44*	-11

2,K,-5

-2	27*	1
-1	29*	-17
0	29*	9
1	31*	2
2	31*	14
3	29*	-28
4	29*	11

2,K,5

-8	47	-44
-7	54	50
-6	45*	-45
-5	45*	44
-4	46*	14
-3	93	-92
-2	89	99
-1	62	-77
0	46*	42
1	45*	-11
2	55	-51
3	89	99
4	54	-71

3,K,-4

-3	26*	17
----	-----	----

-2	37	-27
-1	28*	9
0	28*	18
1	29*	-20
2	39	30
3	54	-40
4	27*	12
5	50	45
6	36*	-43
7	23*	18
8	27	-20

3,K,4

-5	63	-63
-4	35*	16
-3	91	102
-2	67	-74
-1	34*	20
0	35*	-10
1	35*	-14
2	89	75
3	63	-73
4	36*	5
5	36*	33
6	75	-82
7	68	58

APPENDIX IV

List of programs used from the X-Ray System '72.

- BONDAT Generation of bonded atom positions.
- BONDLA Determination of contact and bond distances and angles
 with estimated errors.
- CRYLSQ General crystallographic least squares program.
- DATRDN Preparation of binary data file and preliminary treatment
 of data and symmetry.
- FC Structure factor calculation.
- FOURR Fourier transformations to give Patterson, vector,
 electron density, difference, or E-maps.
- LISTFC Lists structure factors for calculations.
- LOADAT Loading of atomic parameters into the binary data file.
- NORMSF Preliminary data scaling, calculation of quasi-normalised
 structure factors and estimation of overall temperature
 factor.
- RLIST Lists R values for various zones and other reflection classes.

APPENDIX V

The Σ_1 Formula

The Σ_1 formula indicates the signs of centric reflections which are also structure invariants. Its most general form is:

$$S \{ E_{2h2k2l} \} \sim S \{ |E_{hkl}|^2 - 1 \}$$

where $S \{ E_{hkl} \}$ means the sign of E_{hkl}

REFERENCES

- (1) R.E. Marsh, J. Donohue: Adv. in Protein Chem. (1967), 22, 235.
- (2) P. Jose, L.M. Pant: Acta Cryst. (1965), 18, 806.
- (3) K. Torii, Y. Iitaka: Acta Cryst. (1970), B26, 1317.
- (4) M. Mallikarjunan, S.T. Rao: Acta Cryst. (1969), B25, 296.
- (5) O. Ando, T. Asida, Y. Sasada, M. Kakudo: Acta Cryst. (1967), 23, 172.
- (6) S.T. Rao: Z. Kristallographie (1969), 128, 339.
- (7) R.L. Kayushina, B.K. Vainshtein: Kristallografija (1965), 10, 833.
- (8) Y. Mitsui, M. Tsuboi, Y. Iitaka: Acta Cryst. (1969), B25, 2182.
- (9) M.O. Chaney, O. Seely, L.K. Steinrauf: Acta Cryst. (1971), B27, 544.
- (10) J.L. Derissen, H.F. Endeman, A.F. Peerdeman: Acta Cryst. (1968),
B24, 1349.
- (11) S.T. Rao, R. Srinivasan, V. Valambal: Indian J. Pure and Applied
Physics (1968), 6, 523.
- (12) S. Hirokawa: Acta Cryst. (1955), 8, 637.
- (13) D.A. Wright, R.E. Marsh: Acta Cryst. (1962), 15, 54.
- (14) J.J. Madden, E.L. McGandy: Acta Cryst. (1972), B28, 2382.
- (15) P. Edington, M.M. Harding: Acta Cryst. (1974), B30, 204.
- (16) I. Bennett, A.G.H. Davidson, M.M. Harding, I. Morelle: Acta
Cryst. (1970), B26, 1722.
- (17) G.V. Gurskaya, B.K. Vainshtein: Krystallografija (1963), 8, 368.
- (18) G.V. Gurskaya: Kristallografija (1964), 9, 839.
- (19) J. Dow, L.H. Jensen, S.K. Mazumdar, R. Srinivasan, G.N. Ramachandran:
Acta Cryst. (1970), B26, 1662.
- (20) T. Takigawa, T. Ashida, Y. Sasda, M. Kakudo: Bull. Chem. Soc. Jap.
(1966), 39, 2369.

- (21) R.R. Ayyar, R. Chandrasekaran: *Curr.Sci.* (1967), 36, 139.
- (22) M.M. Harding, H.A. Long: *Acta Cryst.* (1968), B24, 1096.
- (23) R.R. Ayyar: *Z. Kristallographie* (1968), 126, 227.
- (24) M.O. Chaney, L.K. Steinrauf: *Amer. Cryst. Assoc., Abstr. Papers* (1969), 21.
- (25) H. Konishi, T. Ashida, M. Kakudo: *Bull. Chem. Soc. Jap.* (1968), 41, 2305.
- (26) W.A. Hendrickson, J. Karle: *Acta Cryst.* (1971), B27, 427.
- (27) W. Cochran, B.R. Penfold: *Acta Cryst.* (1952), 5, 644.
- (28) R. Schaffrin, J. Trotter: *J. Chem. Soc. A* (1970), 25.
- (29) A.R. Kalyanaraman: *Curr. Sci.* (1967), 36, 168.
- (30) S. Guha, S.K. Mazumdar, N.N. Saha: *Z. Kristallographie* (1969), 129, 84.
- (31) A. Chiba, T. Ueki, T. Ashida, Y. Sasada, M. Kakudo: *Acta Cryst.* (1967), 22, 863.
- (32) Y. Iitaka: *Acta Cryst.* (1961), 14, 1.
- (33) B. Oughton, P.M. Harrison: *Acta Cryst.* (1959), 12, 396.
- (34) E. Subramanian: *Acta Cryst.* (1967), 22, 910.
- (35) Y.C. Leung, R.E. Marsh: *Acta Cryst.* (1958), 11, 17.
- (36) V. Pattabhi, K. Venkatesan, S.R. Hall: *Cryst. Struc. Comm.* (1973), 2, 223.
- (37) C.K. Moller: *Acta Chemica Scandinavica* (1949), 3, 1326.
- (38) J. Karle, H. Hauptman: *Acta Cryst.* (1956), 9, 635.
- (39) G. Germain, P. Main, M.M. Woolfson: *Acta Cryst.* (1970), B26, 274.
- (40) G. Germain, P. Main, M.M. Woolfson: *Acta Cryst.* (1971), A27, 368.

- (41) W. Cochran, A.S. Douglas: Proc. Roy. Soc. (1954), A227, 486.
- (42) D.T. Cromer, J.B. Mann: Acta Cryst. (1968), A24, 321.
- (43) S. Abrahamson: J. Sci. Instruments (1966), 43, 931.
- (44) N.L. Xuong: J. Phys. E : Sci. Instruments (1969), 2, 485.
- (45) C.E. Nockolds, R.H. Kretsinger: J. Phys. E : Sci. Instruments (1970), 3, 842.
- (46) P.E. Werner: Acta Cryst. (1970), A26, 489.
- (47) A.M. O'Connell : Acta Cryst. (1967), 23, 623.
- (48) M.J. Buerger : The Precession Method, 19 (Wiley).
- (49) H.S. Kim, G.A. Jeffrey: Acta Cryst. (1969), B25, 2607.

ACKNOWLEDGEMENTS

First and foremost, I should like to express my sincere thanks to my supervisor, Dr. Marjorie Harding, for her continual help and interest throughout this work. I am also grateful to Dr. R.O. Gould for his help with many of the computing problems, and to Dr. C.A. Beevers for some much needed moral support.

My thanks are also due to Mrs. Heather Drummond, for the computer programs written in connection with the processing of the film scanner data, to Dr. D. Green, for supplying the photographs of lactoglobulin, to the Edinburgh Regional Computing Centre for computing facilities, and to Dr. Stewart (University of Maryland) and Dr. P. Main (University of York) for the use of the X-RAY and MULTAN computer programs respectively.

Finally, I wish to acknowledge receipt of financial support from the University of Edinburgh Over the period 1970-1973.